A neuroendocrine pathway modulating osmotic stress in *Drosophila*

Meet Zandawala[1,4,*], Thomas Nguyen[2], Marta Balanyà Segura[3], Helena A. D. Johard[1], Mirjam Amcoff[1], Christian Wegener[3], Jean-Paul Paluzzi[2], and Dick R. Nässel[1,*]

[1] Department of Zoology, Stockholm University, S-10691 Stockholm, Sweden
[2] Department of Biology, York University, Toronto, ON, Canada
[3] Neurobiology and Genetics, Würzburg Insect Research (WIR), Theodor-Boveri-Institute, Biocenter, University of Würzburg, Germany
[4] Present address: Department of Neuroscience, Brown University, Providence, USA

* Correspondence to: Meet Zandawala and Dick R. Nässel
E-mail: meet_zandawala@brown.edu ; dnassel@zoologi.su.se

ORCID for M.Z.: 0000-0001-6498-2208
ORCID for MBS: 0000-0003-0983-4944
ORCID for C.W.: 0000-0003-4481-3567
ORCID for J.P.P.: 0000-0002-7761-0590
ORCID for D.R.N.: 0000-0002-1147-7766

Abstract

Environmental factors challenge the physiological homeostasis in animals, thereby evoking stress responses. Various mechanisms have evolved to counter stress at the organism level, including regulation by neuropeptides. Although much progress has been made on the mechanisms and neuropeptides influencing nutritional stress, relatively little is known about the factors and pathways regulating osmotic and ionic stresses. Here, we uncover the neuropeptide Corazonin (Crz) as a neuroendocrine factor that modulates the release of an osmoregulatory peptide, CAPA, to regulate tolerance to osmotic and ionic stress. Both knockdown of *Crz* and acute injections of Crz peptide impact desiccation tolerance and recovery from chill-coma. Comprehensive mapping of the Crz receptor (*CrzR*) expression identified three pairs of *Capa*-expressing neurons (Va neurons) in the ventral nerve cord that mediate these effects of Crz. We further show that Crz is released during dry starvation (desiccation) and acts to restore homeostasis by inhibiting CAPA release via inhibition of cAMP production in Va neurons. Finally, knockdown of *CrzR* in Va neurons also affects CAPA release, and consequently influences desiccation tolerance and chill-coma recovery, considered proxies for diuretic state. Thus, Crz modulates Va neurons to maintain osmotic and ionic homeostasis, which in turn influences stress tolerance. Taken together with our previous work showing that systemic Crz signaling acts to restore nutrients levels by promoting food search and feeding, we propose that Crz signaling also ensures osmotic homeostasis by inhibiting the anti-diuretic CAPA peptides. Thus, Crz ameliorates stress-associated physiology through systemic modulation of both peptidergic neurosecretory cells and the fat body in *Drosophila*.

Key words: Neuropeptide, peptide hormone, GPCR, stress resistance, Gonadotropin-releasing hormone, neuromedin U, CAPA, osmotic homeostasis

Author summary

Insects are among the largest groups of animals and have adapted to inhabit almost all environments on Earth. Their success in surviving extreme conditions stems largely from their ability to withstand environmental stress, such as desiccation and cold. However, the neural mechanisms that are responsible for coordinating responses to counter these stresses are largely unknown. To address this, we delineate a neuroendocrine axis utilizing the neuropeptides Corazonin (Crz) and CAPA, that coordinate responses to metabolic and osmotic stress. We show that Crz modulates the release of an anti-diuretic peptide, CAPA from a set of neurosecretory cells. CAPA in turn influences osmotic and ionic balance via actions on the Malpighian tubules (the insect analogs of the kidney) and the intestine. Taken together with earlier work, our data suggest that Crz acts to restore metabolic homeostasis at starvation and as a cosenquence of energy mobilization and ensuing metabolic water production, fluid balance needs to be adjusted and therefore CAPA release is inhibited. Hence, this work provides a mechanistic understanding of the neuroendocrine mitigation of metabolic and osmotic stress by two peptide systems.

Introduction

Environmental conditions continuously challenge the physiological homeostasis in animals, thereby evoking stress that can adversely affect the health and lifespan of an individual. For instance, lack of food and water, extreme temperatures, infection and predation can all evoke stress responses. In order to counter this stress and restore homeostasis, animals have evolved a multitude of physiological and behavioral mechanisms, which involve actions of multiple tissues and/or organs (see 1, 2). The core of these mechanisms involves hormones and neuropeptides, which orchestrate the actions of various organs to counteract stress and maintain homeostasis. One well studied mechanism counteracting water-deficit stress is the mammalian anti-diuretic system that involves hypothalamic osmoreceptors stimulating the sensation of thirst that leads to the release of the anti-diuretic hormone vasopressin, which targets multiple organs, including the kidney, to decrease urine output and conserve water (3, 4). In insects such as the vinegar fly, *Drosophila melanogaster,* much progress has been made on the mechanisms and factors regulating metabolic homeostasis, nutritional stress and longevity (see 1, 5-8). Several neuropeptides and peptide hormones have been shown to influence responses to nutrient stress via actions on peripheral tissues such as the liver-like fat body. Specifically, these peptide hormones include *Drosophila* insulin-like peptides (DILPs), adipokinetic hormone (AKH) and corazonin (Crz) (9-16). In addition, mechanisms regulating the release of these hormones are being unraveled (12, 17, 18). Hence, we begin to understand the neural circuits and neuroendocrine pathways regulating metabolic homeostasis, and nutritional stress. However, the circuits and/or pathways that regulate thermal, osmotic and ionic stresses remain largely unexplored.

Thus, we ask what factors and cellular systems constitute the osmoregulatory axis in *Drosophila* (and other insects)? Since nutrient and osmotic homeostasis are inter-dependent (19, 20), we hypothesized that regulation of osmotic stress may involve factors that also regulate nutritional stress. Here, we identified Crz signaling, a paralog of the AKH/Gonadotropin-releasing hormone signaling system (21, 22), as a candidate regulating these stresses. Based on previous research in *Drosophila* and other insects, it has been hypothesized that Crz modulates responses to stress, especially nutritional stress (16, 23, 24). Consistent with this, recent work has shown that neurosecretory cells co-expressing Crz and short neuropeptide F (sNPF) are nutrient sensing (17, 25) and modulate nutrient

115 homeostasis through differential actions of the two co-expressed neuropeptides. Whereas
116 sNPF acts on the insulin-producing cells (IPCs) and AKH-producing cells to stimulate DILP
117 release and inhibit AKH release, respectively, systemic Crz signaling modulates feeding
118 and nutritional stress through actions on the fat body (9, 14, 17).
119
120 Although the role of Crz in regulating responses to nutritional stress is now established,
121 less is known about its role in cold tolerance and ion/water homeostasis. Hence, to
122 address this, we examine the role of Crz in modulating osmotic and ionic stresses and
123 furthermore outline the cellular systems constituting the Crz signaling axis. To this end, we
124 analyzed the effects of manipulating Crz signaling on desiccation tolerance and chill-coma
125 recovery as these two assays are routinely used to assess responses to osmotic/ionic
126 stress (26, 27). Both knockdown of *Crz* and acute injections of Crz peptide impact
127 desiccation tolerance and recovery from chill-coma. Comprehensive mapping of the Crz
128 receptor (*CrzR*) expression revealed that these effects of Crz are not likely mediated by
129 direct modulation of the osmoregulatory tissues but indirectly via three pairs of neurons
130 (Va neurons) in the ventral nerve cord (VNC), which express an osmoregulatory peptide,
131 CAPA. Knockdown of the *CrzR* in Va neurons affects CAPA release and diuresis,
132 consequently influencing desiccation tolerance and chill-coma recovery. Crz acts via
133 inhibition of cAMP production in Va neurons to inhibit release of the anti-diuretic CAPA and
134 thereby allowing for removal of metabolic water produced by energy mobilization, as well
135 as for subsequent post-feeding diuresis. Our data, taken together with published findings
136 (14) suggest that Crz is released into the hemolymph during nutritional stress and acts on
137 the fat body to mobilize energy for food search to increase food intake. In summary, we
138 propose that Crz acts upstream of CAPA signaling to regulate water and ion balance after
139 restoring nutrient levels caused by starvation. Thus, in addition to the hormonal actions of
140 Crz on the fat body to maintain metabolic homeostasis and counter nutritional stress (14),
141 this peptide also helps maintain osmotic homeostasis.
142

143 Results

144 *Crz* knockdown influences osmotic and ionic stresses

145 In adult *Drosophila*, Crz is expressed in two major cell clusters (28): dorsal lateral
146 peptidergic neurons (DLPs) in the pars lateralis of the brain **(S1A Figure)** which co-express
147 sNPF (9) and 2-3 pairs of male-specific interneurons in the abdominal neuromeres of the

148 VNC **(S1B Figure)** (29). The DLPs can be further subdivided into two groups; a pair of large
149 neurosecretory cells and several pairs of smaller neurons in the superior lateral
150 protocerebrum, some of which are neurosecretory while others innervate the antennal lobe
151 **(S1C Figure)**. Previously, we showed that global knockdown of *Crz* (*Crz>Crz-RNAi*)
152 increased survival of flies exposed to desiccation (14). Hence, we asked whether global
153 knockdown of *Crz* also influences chill-coma recovery (CCR) that can be used as a proxy
154 for the diuretic state of the fly. Indeed, knockdown of *Crz* using *Crz-RNAi*$^{\#1}$ **(Figure 1A)** also
155 results in delayed recovery from chill-coma **(Figure 1B)** and also increased survival under
156 ionic stress **(Figure 1C)**.
157

158 **Crz peptide injections influence desiccation survival and chill-coma recovery**

159 Having shown that chronic genetic manipulations that interfere with Crz signaling impacts
160 stress tolerance, we asked whether acute increase of Crz signaling also affects these stress
161 responses. To this end, we first quantified the recovery time of flies from chill-coma that had
162 been injected with Crz. An injection of a high dose of Crz (10^{-6}M), but not a low dose (10^{-}
163 ^{9}M), delays recovery from chill-coma **(Figure 1D)**. These effects are not due to changes in
164 osmolarity since injection of an inactive exogenous peptide (non-amidated *Aedes aegypti*
165 ACP, naACP) has no effect on chill coma recovery **(Figure 1E)**. Next, we independently
166 assayed the Crz-injected flies for survival under desiccation conditions. Flies injected with
167 10^{-6}M Crz display decreased desiccation tolerance compared to saline-injected flies **(Figure**
168 **1F)**. Taken together, these results suggest that Crz decreases resistance to desiccation and
169 cold exposure.
170

171 ***CrzR* is expressed in CAPA and other peptidergic neurons**

172 Since Crz signaling influences osmotic and ionic stresses, we wanted to outline the
173 pathways mediating this response. We predicted that Crz may modulate these stresses via
174 either directly acting on peripheral tissues such as the Malpighian tubules (analogous to the
175 human kidney) and/or hindgut and rectum that regulate ionic and water homeostasis, or
176 indirectly through one (or more) of the diuretic/anti-diuretic peptide hormones that act on
177 these organs. To determine the mode of Crz action, we examined expression of the *CrzR* in
178 the CNS and peripheral tissues by driving GFP expression using different *CrzR-GAL4* lines.
179 *CrzR-GAL4*^{T11a} and *CrzR-GAL4*^{Se} had similar expression patterns; however, *CrzR-GAL4*^{T11a}
180 resulted in stronger GFP expression than *CrzR-GAL4*^{Se} (data not shown). Hence, the *CrzR-*

181 *GAL4^{T11a}* line (referred to as *CrzR-GAL4* from hereon) was used for all the subsequent
182 experiments. In the periphery, *CrzR* is not expressed in the midgut, hindgut or Malpighian
183 tubules **(S2A Figure)**. However, weak *CrzR* expression is present in sparse efferent
184 neuronal projections to the rectal pad **(S2B Figure)**. Overall, this is consistent with the RNA-
185 Seq expression of *CrzR* reported on FlyAtlas 2 **(S2C Figure)**; however, these findings
186 suggest that the effects of Crz on diuresis, and thus ionic and osmotic stress tolerance, are
187 likely mediated via another neuropeptide and not by direct actions on peripheral osmo- and
188 ionoregulatory tissues.
189
190 In *Drosophila*, there are four main neuropeptides (primarily diuretic) that are known to
191 influence water and ionic homeostasis via direct actions on peripheral tissues: CAPA,
192 diuretic hormone 44 (DH44), diuretic hormone 31 (DH31) and leucokinin (LK) (see 6). As a
193 first step to determine if any of these neuropeptides act downstream of Crz signaling, we
194 comprehensively mapped the distribution of *CrzR* in the adult CNS and co-labelled these
195 specimens with antibodies against various neuropeptides. Within the adult brain, *CrzR* is
196 expressed in distinct cell clusters **(S3A Figure)** and branches of these neurons partly
197 superimpose the Crz-expressing DLP neuron processes **(S3B-C Figures)**. In the adult
198 VNC, the *CrzR* is strongly expressed in three pairs of neurons in the abdominal neuromeres
199 A2-A4 **(S3D Figure)**. In addition, weak GFP expression is also observed in two pairs of
200 posterior neurons (indicated by a white arrow). These might be the efferent neurons that
201 innervate the rectal pad **(S2B Figure)**. Using peptide immunolabeling we found that *CrzR* is
202 expressed in a single pair of neurons in the SEZ and three pairs of Va neurons in the VNC,
203 which express the *Capa* gene (*Capa* encodes CAPA-1, CAPA-2 and pyrokinin-1 (PK-1)
204 neuropeptides) **(Figure 2)** (30-32). In addition, *CrzR* is weakly expressed in a subset of the
205 six DH44-expressing median neurosecretory cells in the pars intercerebralis **(S4 Figure)**.
206 However, *CrzR* expression was not detected in neurons expressing DH31 **(S5A-C Figures)**
207 or LK **(S5D-F Figures)**. CAPA peptides produced by the Va neurons have been previously
208 implicated in affecting tolerance to desiccation and cold via actions on the Malpighian
209 tubules (26). Moreover, as a result of differential prohormone processing, the *CAPA* gene
210 expressing neurons in the SEZ only produce a pyrokinin-1 neuropeptide, whereas the Va
211 neurons can produce all three peptides encoded by *CAPA* (32). Since DH44 knockdown
212 has no effect on desiccation tolerance (33), and since we detected strong *CrzR* expression
213 in Va neurons but not DH44 neurons, we focus here on the Crz-CAPA pathway, specifically

214 the CAPA-expressing Va neurons. To further validate *CrzR* expression in Va neurons, we
215 utilized a recently generated *CrzR-T2A-GAL4* line where the T2A-GAL4 encoding cassette
216 is inserted immediately upstream of the stop codon of *CrzR* (34). As expected, *CrzR-T2A-*
217 *GAL4* also drove GFP expression in Va neurons (data not shown) further supporting the link
218 between Crz and CAPA.
219
220 Additionally, we tried to identify potential interactions between Crz and other neurons
221 producing feeding and stress-regulating peptides using a similar approach. The *CrzR* is not
222 expressed in insulin-producing cells **(S6A Figure)** or AKH-producing cells **(S6B Figure)**,
223 consistent with previous data identifying sNPF as the functional neurotransmitter in DLPs
224 affecting DILP and AKH release (17). Interestingly, *CrzR* is expressed in a subset of the
225 *Hugin*-producing neurons (35) in the SEZ **(S6C Figure)**, as well as neurons in the SEZ
226 reacting with antiserum to FMRFamide (this antiserum cross reacts with neuropeptides such
227 as sNPF, NPF, sulfakinin, FMRFamide and myosuppressin, which all have an RFamide C-
228 terminus) **(S6D Figure)**. Furthermore, *CrzR* was detected in PDF-expressing small
229 ventrolateral clock neurons (sLNvs) (36) **(S6E-F Figures)**. The Hugin neuropeptide (Hugin-
230 PK) has been shown to regulate feeding and locomotion in larval and adult *Drosophila* (37-
231 39) and PDF-expressing sLNvs are part of the circadian clock circuit (40, 41).
232
233 **Crz inhibits cAMP levels in Va neurons**
234 Having shown that *CrzR* is expressed in Va neurons, we asked whether Va neurons can
235 respond directly to Crz. Since the identity of the second messengers utilized by CrzR is
236 unknown, we first predicted the coupling specificity of CrzR to various G-proteins
237 (http://athina.biol.uoa.gr/bioinformatics/PRED-COUPLE2/) (42). This analysis revealed high
238 coupling specificity of CrzR to Gi/o G-protein (p-value = 1.69×10^{-6}) suggesting that Crz
239 may inhibit the cAMP dependent pathway. Consistent with this prediction, bath application
240 of Crz to dissected VNC diminished NKH477 ((a forskolin analog and potent adenylyl
241 cyclase activator) stimulated cAMP levels in Va neurons**)**, indicated by the response of the
242 FRET-based cAMP sensor Epac1-camps **(Figures 3A-D**. Addition of Crz alone had no
243 impact on the cAMP FRET signal compared to saline controls **(Figures 3A-B)**. However,
244 either an addition of NKH477 to preparations pre-incubated with Crz **(Figures 3A-B)** or
245 simultaneous coapplication of Crz and forskolin **(Figures 3C-D)** resulted in a reduced cAMP
246 FRET signal compared to their respective controls. In addition, Crz application to *ex vivo*

247 preparations had no impact on Ca^{2+} levels in Va neuron as measured using GCaMP
248 fluorescence **(Figures 3E-F)**. These results suggest that Crz inhibits cAMP levels in Va
249 neurons, most likely by direct action on the CrzR.
250
251 We next asked what the neuronal source of Crz is and whether its mode of action on Va
252 neurons is systemic via the circulation or synaptic/paracrine within the abdominal
253 neuromeres. To address this, we examined the morphology of Crz and CAPA neurons. As
254 described above, Crz is expressed in the DLPs, and in males, in abdominal ganglion
255 interneurons **(S1 Figure)**. The DLPs do not have axonal projections descending into the
256 VNC but they send axons to the corpora cardiaca (CC), anterior aorta and intestine (9, 43).
257 Thus, Crz can be released into the hemolymph and is likely to act hormonally on Va
258 neurons. The male-specific Crz interneurons in the abdominal neuromeres, on the other
259 hand, could potentially interact with Va neurons via superimposed processes, at least in a
260 paracrine fashion **(S7A Figure)**. However, the fact that *CrzR* expression is also detected in
261 Va neurons of females **(S7B-C Figures)** suggests that the Crz-CAPA pathway is not
262 restricted to males. Thus, the DLPs, that are present in both sexes, appear to be the source
263 of hormonal Crz, modulating the Va neurons.
264

265 **Release of Crz and CAPA peptides is altered under desiccation conditions**

266 Next, we sought to determine whether Crz is released from the DLPs into the hemolymph
267 during stress and how this in turn affects the release of CAPA from Va neurons. We utilized
268 Crz-immunoreactivity as a measure of peptide release; a decrease in Crz-immunoreactivity
269 would indicate increased peptide release assuming there is no change in peptide
270 production. The Crz immunoreactivity levels were quantified both in the large DLP neurons
271 separately and also in all DLPs together, to see if there is a functional difference between
272 these subpopulations **(Figure 4A)**. Interestingly, the Crz peptide level in the large DLP
273 neurons was significantly reduced in desiccated and rewatered flies **(Figure 4A and B)**
274 whereas the peptide level in all Crz neurons displayed a reduction in starved flies as well
275 **(Figure 4A and S8A Figure)**. Since *Crz* transcription (a proxy for Crz peptide production)
276 remains constant under osmotic **(Figure 4E)** and nutritional **(S8B Figure)** stresses, these
277 results imply that there is stress-dependent release of Crz from the two subclasses of DLPs,
278 albeit the cell-specific release varies depending on the type of stress.

279 Using a similar approach, we also quantified CAPA peptide levels in the Va neurons. We
280 found that the CAPA immunoreactivity is unaltered by desiccation of the flies, but
281 significantly higher in rewatered flies **(Figure 4C and D)**. Levels of *Capa* transcript, on the
282 other hand, is higher following desiccation and returns back to normal after rewatering
283 **(Figure 4F)**. Unlike its role during osmotic stress, both the *Capa* transcript **(S8C Figure)**
284 and peptide levels **(Figure 4C and D)** are unaltered following starvation and refeeding
285 indicating it is not involved in nutritional stress. Thus, under desiccation, CAPA production
286 and release are both increased, resulting in no net difference in immunoreactivity. Following
287 rewatering, CAPA production is lowered and its release is inhibited resulting in increased
288 CAPA immunoreactivity. Given that *Crz* knock down led to increased chill-coma recovery
289 time **(Figure 1B)**, we examined if *Crz* levels changed after chilling. Compared to normal
290 flies, chilling and recovered flies demonstrated no change in *Crz* transcript levels **(Figure**
291 **4G)**, whereas comparatively, *Capa* transcript levels were significantly decreased in
292 response to chilling and returned to normal levels when flies were allowed to recover at
293 room temperature after chilling **(Figure 4H)**.
294

295 **Crz signaling to Va neurons affects tolerance to osmotic stress**

296 Since our imaging data indicates expression of *CrzR* in CAPA-producing Va neurons, and
297 that Crz might inhibit CAPA release, we next examined the functional interaction between
298 Crz signaling and Va neurons. To accomplish this, we utilized two independent GAL4 lines
299 (*Va-GAL4* and *CAPA-GAL4*) to knock down the *CrzR* in Va neurons. Since both the *CrzR-*
300 *RNAi* lines [*CrzR-RNAi (1)* and *(2)*] tested are equally effective at knocking down *CrzR,* we
301 utilized *CrzR-RNAi (1)* (referred to as *CrzR-RNAi* from hereon) for all the experiments **(S8D**
302 **Figure)**. The *Va-GAL4* is stronger (based on the intensity of GFP expression) and drives
303 expression in a broader set of neurons compared to *CAPA-GAL4*. The *Va-GAL4* is
304 expressed in several neurons in the brain and VNC in addition to the *CAPA* expressing
305 neurons (**S9A-B Figures)**, whereas the *CAPA-GAL4* is only expressed in a pair of CAPA-
306 negative brain neurons **(S9C Figure)** and the Va neurons in the VNC **(S9D Figure)**. Using
307 these two drivers, we asked whether knockdown of *CrzR* in Va neurons impacts CAPA
308 release and consequently the phenotypes associated with CAPA signaling. If Crz inhibits
309 CAPA release, knock down of *CrzR* in Va neurons should relieve this inhibition and result in
310 increased CAPA release. Consistent with this prediction, *Va-GAL4* driven *CrzR-RNAi*
311 indeed results in decreased CAPA peptide levels in Va neurons **(Figure 5A)**, indicating

312 increased CAPA release. We next asked what role does CAPA play following its release
313 into the hemolymph? While originally identified as a stimulator of fluid secretion in
314 *Drosophila* (44), there have been conflicting reports on the roles of CAPA signaling in
315 insects acting as either a diuretic or an anti-diuretic hormone, or having no effect on fluid
316 secretion (26, 27, 45, 46). However, recent reports suggest that at physiologically relevant
317 concentrations, CAPA is an anti-diuretic and increased CAPA-signaling results in delayed
318 recovery from chill-coma *in vivo* as well as a reduction in *ex vivo* secretion by Malpighian
319 tubules (27, 47). To determine whether CAPA acts as an anti-diuretic *in vivo*, we monitored
320 the excretion rate of flies in which CAPA neurons were thermogenetically activated using
321 ectopically expressed *TRPA1* channel. Consistent with the *ex vivo* data, *CAPA>TRPA1* flies
322 display reduced excretion rates compared to control flies **(Figure 5B)**. This reduced
323 excretion could be mediated via actions on the gut and Malpighian tubule principal cells,
324 which express the CAPA receptor (*CAPAR)* **(S11 Figure)**. Our findings, thus, suggest that
325 CAPA acts as anti-diuretic *in vivo*.
326
327 Additionally, if knockdown of *CrzR* in Va neurons results in increased CAPA release, we
328 should observe the same phenotypes for *Va>CrzR-RNAi* as one would following increased
329 CAPA signaling. Indeed, *Va-GAL4* driven *CrzR-RNAi*, which causes increased CAPA
330 signaling, results in delayed recovery from chill-coma **(Figure 5C)** and increased survival
331 during desiccation **(Figure 5D)** and ionic stress **(Figure 5E)**, consistent with the role of
332 CAPA as an anti-diuretic. In addition, we observed increased survival under starvation
333 **(Figure 5F)**, possibly due to effects on food intake as a result of *CrzR* knockdown in non-
334 CAPA expressing neurons **(S10 Figure)**. Hence, we knocked down the *CrzR* more
335 selectively using *CAPA-GAL4*. The *CAPA-GAL4* driven *CrzR-RNAi* resulted in increased
336 survival under desiccation **(Figure 5G)**. However, it did not have any impact on chill-coma
337 recovery **(Figure 5H)**. Similar results were also obtained by knocking down *CrzR* in CAPA
338 neurons using an independent *CrzR-RNAi* construct *CrzR-RNAi (2*). The lack of effect on
339 chill-coma recovery following *CrzR* knockdown with *CAPA-GAL4* could be due to it being a
340 very week driver. Taken together, our data indicate that Crz acts on Va neurons to inhibit
341 the release of an anti-diuretic hormone CAPA, and thereby affecting tolerance to osmotic
342 and ionic stresses.
343
344

Discussion

We have found here that a peptidergic neuroendocrine pathway in *Drosophila*, known to restore nutrient deficiency (utilizing Crz), integrates a further peptidergic component (CAPA) to maintain osmotic and ionic homeostasis **(Figure 6)**. The Crz-CAPA signaling thereby also influences tolerance to osmotic and cold stress. An earlier study suggested that Crz is released during nutritional stress to mobilize energy stores from the fat body to fuel food search behavior (14). Furthermore, that study suggests that increased Crz signaling compromises resistance to starvation, desiccation and oxidative stress (14). We confirm these findings here, and also find that Crz inhibits a set of *CrzR* expressing Va neurons in the abdominal ganglia that produce anti-diuretic CAPA peptides.

The *Capa* gene-derived neuropeptides (CAPA1 and CAPA2) are well established as osmoregulatory factors that act on the Malpighian tubule principal cells (see 45, 48) and perhaps the hindgut, as indicated herein by our receptor expression data. Previous studies showed that CAPA neuropeptides act as diuretic hormones in *Drosophila* and other dipterans (30, 49). However, other recent work has provided evidence to suggest that CAPA neuropeptides are anti-diuretic, also in *Drosophila* (27, 46, 50). Our findings herein also support an anti-diuretic role of CAPA peptides. Furthermore, we show that the CAPA-producing Va neurons are downstream of Crz signaling and we propose that under harsh conditions when flies are exposed to dry starvation (desiccation without food) the two signaling systems act in tandem to restore homeostasis. The exposure to desiccation results in increased hemolymph osmolarity, and the fly responds acutely by releasing anti-diuretic CAPA (and maybe other anti-diuretic hormones) to preserve water (20). As the dry starvation continues, the nutrients diminish in the fly, and nutrient sensors record this deficiency, which triggers release of hormones that act to restore metabolic homeostasis. As indicated above, one such hormone is Crz, known to provide energy for food search and induce feeding (14, 16). Mobilization of energy, especially in the form of stored lipids, yields metabolic water and metabolites (see 51, 52, 53) that need to be excreted and thus diuresis needs to be diminished. In insects, increased food intake also yields water (see 54), which requires post-feeding diuresis to restore water homeostasis. The increased need for excretion means that the anti-diuretic action of CAPA needs to be terminated. We propose that onset of Crz release is likely to be induced later than that of CAPA peptides at dry starvation and results in inhibition of the Va neurons and hence diminished CAPA release.

378 Thus, both nutrient and water homeostasis can be restored. Unfortunately, there is no
379 method sensitive enough to monitor the timing of changes in hemolymph levels of Crz and
380 CAPA in small organisms such as *Drosophila*. Indirect measurements, like monitoring levels
381 of peptide-immunolabel in neurons of interest are not necessarily accurate, since these
382 levels reflect the "balance" between peptide release and production and therefore not useful
383 for resolving onset and duration of release with accuracy.
384
385 Our evidence for the Crz action on CAPA-producing Va neurons is based on the expression
386 of *CrzR* in these cells, as well as functional imaging data which shows that Crz inhibits
387 cAMP production in Va neurons (but has no impact on intracellular Ca^{2+} levels). This led us
388 to investigate the effects of manipulating Crz signaling and targeted *CrzR* knockdown in Va
389 neurons on aspects of water and ion homeostasis and cold tolerance, which have been
390 shown earlier to be affected by CAPA signaling (26, 27). Previous work demonstrated that
391 *in vivo* injections of physiological levels of CAPA peptide compromises chill tolerance,
392 including increased chill-coma recovery (CCR) time and survival following prolonged cold
393 stress (27). These physiological effects also mirror the action of CAPA on diuresis as well
394 as water and ionic stress. Thus, our observations that *Crz* or *CrzR* knockdown leads to
395 increased CCR time (i.e. jeopardizing cold tolerance) and increased tolerance to ionic stress
396 are in line with the results of CAPA injections shown before (27). Furthermore, our
397 experiments that target knockdown of *CrzR* to Va neurons also affected CCR, and tolerance
398 to starvation, desiccation, and ionic stress. Injecting flies *in vivo* with Crz in the present
399 study also resulted in effects on CCR and survival during desiccation, further strengthening
400 our model in which Crz modulates release of CAPA.
401
402 Previous work in *Drosophila* showed that not only does global *Crz* knockdown result in
403 increased resistance to starvation, desiccation and oxidative stress, but also found that
404 *CrzR* knockdown in the fat body (and salivary glands) led to these same phenotypes (9, 14).
405 These findings suggest that Crz signaling to the fat body accounts for some of the stress
406 tolerance phenotypes seen following *Crz* knockdown. Thus, it is possible that the effects
407 observed on desiccation survival following Crz peptide injections in the present study are
408 partly confounded by the actions of this peptide on the fat body and other tissues
409 expressing the CrzR.
410

411 Earlier data show that after *CrzR* knockdown in the fat body, glucose, trehalose and
412 glycogen levels are elevated in starved flies, but not in normally fed flies (14). Moreover,
413 starved, but not normally fed flies with *Crz* knockdown, display increased triacyl glycerides
414 (9) and *Crz* transcript is upregulated in starved flies with *CrzR* knockdown in the fat body
415 (14). This further emphasizes that systemic Crz signaling is critical under nutritional stress.
416 Our data on Crz immunolabeling intensity corroborate these earlier findings and suggest
417 that Crz is released to restore metabolic homeostasis by mobilizing energy stores from the
418 fat body to fuel food search behavior, and after restoring osmotic stress the peptide acts to
419 down-regulate CAPA release from Va neurons.
420
421 We did not address the question as to how the Crz neurons sense nutrient deficiency or
422 whether they can detect changes in osmolarity. However, it is known that Crz-producing
423 DLPs express an aquaporin, Drip, and the carbohydrate-sensing gustatory receptors, Gr43a
424 and Gr64a (55-57). A subset of the Crz neurons also express a glucose transporter (Glut1)
425 that is involved in glucose-sensing (Oh et al., 2019). Thus, imbalances in internal nutritional
426 and maybe even osmotic status could either be sensed cell autonomously by the Crz
427 neurons or indirectly by signals relayed to them via other pathways.
428
429 A few other findings might support roles of Crz in ameliorating nutrient stress. We found
430 here that Crz neurons innervate the antennal lobe (AL)**,** and that the *CrzR* is strongly
431 expressed in local interneurons of the AL. Possibly, Crz modulates odor sensitivity in hungry
432 flies to increase food search, similar to peptides like short neuropeptide F (sNPF),
433 tachykinin and SIFamide (58-60). Another peptide hormone, adipokinetic hormone (AKH),
434 has been shown to be critical in initiating locomotor activity and food search in food deprived
435 flies (13, 15, 61) and AKH also affects sensitivity of gustatory neurons to glucose (62, 63).
436 The effect of AKH on increasing locomotor activity is evident only after 36h of starvation (61)
437 and may correlate with the proposed action of Crz during starvation (see 14). Possibly Crz
438 acts in concert with AKH to allocate fuel during metabolic stress (61). Since we found that
439 the *CrzR* is not expressed in AKH-producing cells, it is likely that these two peptides act in
440 parallel rather than in the same circuit/pathway. However, the DLPs also produce sNPF (9)
441 and this peptide is known to act on the AKH producing cells and thereby modulate glucose
442 homeostasis and possibly, sensitivity of gustatory neurons (17, 19, 62). Thus, the DLPs may

443 act systemically with Crz and by paracrine signaling in the corpora cardiaca to act on AKH
444 cells. Thereby the Crz and AKH systems could be linked by sNPF.
445
446 In conclusion, we suggest that Crz regulates acute metabolic stress-associated physiology
447 and behavior via the fat body to ensure nutrient allocation to power food search and feeding
448 during prolonged starvation. Following energy mobilization and ensuing production of
449 metabolic water, Crz acts to downregulate signaling with anti-diuretic hormone to ensure
450 restoration of water and ion homeostasis. Thus, Crz inhibits the Va neurons to diminish
451 release of CAPA peptides. Taken together, our findings and those of previous studies
452 indicate that Crz acts on multiple neuronal and peripheral targets to coordinate and sustain
453 water, ion and metabolic homeostasis. It might even be possible that an ancient role of the
454 common ancestor of Crz and AKH signaling systems was to modulate stress-associated
455 physiology and that these paralogous signaling systems have sub-functionalized and neo-
456 functionalized over evolution (22, 64).
457
458
459

460 ## Experimental procedures

461 ### Fly lines and husbandry

462 *Drosophila melanogaster* strains used in this study are listed in **Table 1**. Flies were
463 backcrossed into the same genetic background (w^{1118}) for 7 generations, with exception of
464 the stocks used for imaging and defecation assays. All stocks were stored at 18°C under
465 normal photoperiod (12 hours light: 12 hours dark; 12L:12D) on a standard
466 cornmeal/molasses/yeast diet. Unless indicated otherwise, experimental flies were reared
467 under non-crowded conditions and maintained under normal photoperiod at 25°C on
468 enriched medium containing 100 g/L sucrose, 50 g/L yeast, 12 g/L agar, 3 ml/L propionic
469 acid and 3 g/L nipagin. Adult males 6-7 days old post-eclosion were used unless mentioned
470 otherwise.

471

472

473

474 **Table 1**: Fly strains used in this study

Fly strain	Inserted on chromosome	Source / reference	Stock number
CrzR-GAL4 ^{T11a}		From Dr. Jae Park; (65)	
CrzR-GAL4^{Se}		From Dr. Jae Park; (65)	
CrzR-T2A-GAL4		From Dr. Yuko Shimada-Niwa; (34)	
Va-GAL4		From Dr. Stefan Thor (66)	
CAPA-GAL4	II	BDSC; (67)	51969
CAPAR-GAL4		From Dr. Shireen Davies; (68)	
Crz^{1}*-GAL4*		From Dr. Jae Park; (69)	
Crz^{2}*-GAL4*	II	BDSC; (29)	51976
Actin5C-GAL4/Cyo	II	BDSC	4414
UAS-CrzR-RNAi GD (#1)	III	VDRC	44310
UAS-CrzR-RNAi KK (#2)	II	VDRC	108506
UAS-Crz-RNAi GD (#2)	II	VDRC	30670
UAS-Crz-RNAi KK (#1)	II	VDRC	106876
w^{1118} (RNAi control)		BDSC	
yw; Sco/Cyo; UAS-mcd8-GFP	III	BDSC	
JFRC81-10xUAS-IVS-Syn21-GFP-p10 (referred to as 20X GFP)		From Dr. Michael Texada (70)	
20xUAS-IVS-GCaMP6m	II	From Dr. Orie Shafer (71)	
UAS-epac1-camps(50A)	II	From Dr. Orie Shafer (72)	
UAS-TRPA1	II	Würzburg stock collection	

475

476 **Immunohistochemistry and imaging**

477 Immunohistochemistry for *D. melanogaster* adult CNS and gut was performed as described
478 earlier (33). Briefly, tissues were dissected in phosphate buffered saline (PBS), fixed in 5%
479 ice-cold paraformaldehyde (3.5-4 hours), washed in PBS and incubated in primary
480 antibodies (**Table 2**) diluted in PBS with 0.5% Triton X (PBST) for 48 hours at 4°C**.** Samples

481 were then washed with PBST and incubated in secondary antibodies (**Table 2**) diluted in
482 PBST for 48 hours at 4°C. Finally, samples were washed with PBST and then PBS before
483 being mounted in 80% glycerol. Zeiss LSM 780 confocal microscope (Jena, Germany) was
484 used to image all the samples.
485
486 To quantify peptide levels in flies exposed to various stressors, adult males were transferred
487 to either an empty vial (desiccation) or a vial containing aqueous 0.5% agar (starvation) or
488 artificial diet (normal food) and incubated for 18 hours. In addition, one set of flies were
489 desiccated for 15 hours and then transferred to a vial containing 0.5% agar (re-watered) for
490 3 hours. These flies were then processed for immunohistochemistry as described above.
491 Cell fluorescence was quantified as described previously (33). Note that the anti-CAPA
492 antibody used to quantify CAPA peptide levels cross-reacts with other PRXamide-related
493 peptides. Hence, this approach measures the levels of all PRXamide peptides that are
494 coexpressed in a given neuron.
495
496 Confocal images were processed with Fiji (73) for projection of z-stacks, contrast and
497 brightness, and calculation of immunofluorescence levels. Further adjustments (cropping
498 and brightness) were made in Microsoft Powerpoint.
499
500 **Table 2**: Antibodies used for immunohistochemistry

Antibody	Immunogen	Source / reference	Dilution
Primary antibodies			
Rabbit anti-PVK-2 (referred to as anti-CAPA in text)	*Periplaneta americana* CAPA-PVK-2	Dr. Reinhard Predel (74)	1:4000
Rabbit anti-CAPA-2	*Rhodnius prolixus* CAPA-2	Dr. Ian Orchard (27)	1:1000
Rabbit anti-Crz	*Drosophila* Crz	Dr. Jan Veenstra (75)	1:4000
Rabbit anti-DILP2	*Drosophila* DILP2	Dr. Jan Veenstra (76)	1:2000
Rabbit anti-AKH	*Drosophila* AKH	Dr. Mark Brown (77)	1:1000
Rabbit anti-	FMRFamide	Dr. Cornelis	1:4000

FMRFamide		Grimmelikhuijzen (78)	
Rabbit anti-PDH/PDF	Crab *Uca pugilator* pigment dispersing hormone	Dr. Heinrich Dircksen (79)	1:4000
Rabbit anti-LK	*Leucophaea maderae* kinin I	(80)	1:2000
Rabbit anti-DH44	*Drosophila* DH44	(81)	1:1000
Rabbit anti-DH31	*Drosophila* DH31	(82)	1:1000
Mouse anti-GFP	Jelly fish GFP	Invitrogen	1:1000
Chicken anti-GFP	Jellyfish GFP	Invitrogen	1:1000
Mouse anti-nc82	*Drosophila* bruchpilot	DSHB	1:20
Secondary antibodies			
Goat anti-mouse Alexa 488	-	Invitrogen	1:1000
Goat anti-rabbit Alexa 546	-	Invitrogen	1:1000
Goat anti-chicken Alexa Fluor 488	-	Life Technologies	1:1000
Goat anti-mouse Alexa Fluor 546	-	Life Technologies	1:1000
Donkey anti-rabbit Alexa Fluor 647		Life Technologies	1:1000
Goat anti-rabbit Cyanine5	-	Life Technologies	1:500
Other fluorophores			
Rhodamine-phalloidin	-	Invitrogen	1:1000

501

502 **Stress resistance assays**

503 Flies were assayed for survival under desiccation, starvation and ionic stress by being kept
504 in empty vials, vials containing 0.5% aqueous agarose (A2929, Sigma-Aldrich), and vials

505 containing artificial food supplemented with 4% NaCl, respectively. Flies were kept in vials
506 and their survival recorded every 3 to 6 hours until all the flies were dead. The vials were
507 placed in incubators at 25°C under normal photoperiod conditions (12L:12D). For chill-coma
508 recovery of transgenic flies, flies were incubated at 0°C for 4 hours and then transferred to
509 room temperature (24°C) to monitor their recovery time. At least three biological replicates
510 and two technical replicates (10-15 flies per technical replicate) for each biological replicate
511 were performed for each experiment.
512

513 **Peptide injection experiments**

514 *Drosophila* w^{1118} males 7-8 days post-eclosion were used for these experiments. These flies
515 were reared and maintained at room temperature (~23°C).
516

517 ***Peptide Injections***

518 *D. melanogaster* Crz (pQTFQYSRGWTN-NH_2) was custom synthesized at >95% purity by
519 Genscript (Piscataway, NJ, USA); a non-amidated adipokinetic hormone/corazonin-related
520 peptide (naACP) from *Aedes aegypti* (pQVTFSRDWNA), as previously described (83), was
521 custom synthesized at >90% purity by Pepmic Co. (Suzhou, Jiangsu, China). Peptides were
522 initially solubilized in nuclease-free deionized water or DMSO to a stock concentration of 10^{-}
523 ^{3} M and then each peptide was diluted in *Drosophila* saline injection buffer (NaCl 117.5 mM,
524 KCl 20 mM, $CaCl_2$ 2 mM, $MgCl_2$ 8.5 mM, $NaHCO_3$ 10.2 mM, NaH_2PO_4 4.3 mM, HEPES 15
525 mM, glucose 20 mM, pH 6.7) as described previously (26) and supplemented with 0.1%
526 (w/v) Fast Green FCF, which was used to visually confirm successful injections. Peptide
527 injection solutions were prepared to achieve final concentrations in the hemolymph of either
528 10^{-6} or 10^{-9} M and based on the *Drosophila* hemolymph volume of 80 nL (84). Peptide
529 injections took place at room temperature under light CO_2 anesthesia, with injections
530 directed to the left mesopleuron using a micromanipulator-controlled Drummond Nanoject
531 Injector set to 18.4 nL per injection. Control flies received only *Drosophila* saline injection
532 buffer containing 0.1% Fast Green FCF.
533

534 ***Chill-Coma Recovery***

535 Flies were taken from the *Drosophila* vials and lightly anesthetized by CO_2. Once
536 immobilized, male flies were isolated and placed into a white plastic weighing dish that was

537 held over ice. For each treatment, 9-15 males were selected per treatment. After injections,
538 flies were transferred individually into 7.5 mL glass vials that were then submerged in a 0°C
539 ice-water slurry for 1 hour. Afterwards, vials were removed from the slurry and gently dried.
540 Flies were left to recover at room temperature without being disturbed for the duration of the
541 experiment. Recovery was recorded by measuring the time when a fly stands on all legs.
542 Experiments were repeated in at least two independent biological replicates.
543
544 ***Desiccation***
545 As above, male flies were isolated and placed over ice within a white plastic weighing dish.
546 For each treatment, 11-15 males were used. After injection with saline injection buffer alone
547 or buffer containing Crz, all flies in that treatment group were transferred *en masse* into
548 empty *Drosophila* vials without any food or water. Survival under this desiccation treatment
549 was monitored at regular intervals. This experiment was repeated in three replicates.
550
551 **Calcium and cAMP imaging of Va neurons**
552 The whole CNS of feeding 3rd instar larvae expressing the calcium sensor GCaMP6m
553 (Chen, Wardill et al. 2013) or the cAMP sensor Epac1-camps (Shafer, Kim et al. 2008) were
554 dissected in HL3.1 saline ((85), pH 7.2-7.4) and attached at the bottom of a plastic Petri dish
555 lid (35x10 mm; Greiner Bio-One International GmbH, Austria) filled with HL3.1. The CNS
556 was allowed to settle for 10 min and then imaged on a widefield fluorescent imaging setup
557 (for calcium imaging: Zeiss AxioExaminer D1, equipped with a W "Plan-Apochromat"
558 x20/1.0 and a Chroma-ET GFP filter, a pco.edge 4.2 sCMOS camera and a SPECTRA-4
559 light engine; for cAMP imaging: Zeiss Axioskop FS2, equipped with a ZeissPhotometrics
560 DualView2 with Chroma ET-CFP and ET-YFP emission filters and a dualband CFP/YFP
561 dichroic mirror, a CoolSnap CCD camera and a VisiChrome monochromator; both systems
562 from Visitron, Puchheim, Germany).
563
564 For calcium imaging, an excitation wavelength of 475 nm and an exposure time of 180 ms
565 at 2x binning was used. Imaging was performed for 15 min at 1 Hz. After 350 seconds, 10
566 µM (end concentration) synthetic Crz dissolved in HL3.1 containing 0.1% DMSO or HL3.1
567 plus 0.1% DMSO (control) was added. For data analysis, background was subtracted and
568 the change in fluorescence intensity was calculated as $\Delta F/F_0 = (F_n-F_0)/F_0$ were F_n is the
569 fluorescence at time point n and F_0 is the mean baseline fluorescence value of the 30 s

570 before peptide/control application. For cAMP imaging, an excitation wavelenght of 434/17
571 nm and an exposure time of 800 ms at 4x binning was used. Imaging was performed for 80
572 minutes at 1 Hz. In the first set of experiments, 10 μM synthetic Crz dissolved in HL3.1
573 containing 0.1% DMSO or HL3.1 plus 0.1% DMSO (control) was added after 40 min. At 75
574 minutes, 100 μM of the membrane-permeable adenylyl cyclase activator NKH477 (Merck
575 Millipore) was added. In the second set of experiments, 100 μM NKH477 in 0.1% DMSO
576 alone or in combination with 10 μM Crz was added. For data analysis, backgrounds were
577 subtracted and the CFP/YFP ratio was calculated for each time point with a YFP signal
578 corrected for spill-over.
579
580 **Quantitative PCR**
581 ***CrzR-RNAi Knockdown Efficiency***
582 Total RNA was isolated from whole male flies using Quick-RNA™ MiniPrep (Zymo
583 Research) from four independent biological replicates with 8-15 flies in each replicate. The
584 RNA concentration was determined using NanoDrop 2000 spectrophotometer (Thermo
585 Scientific). RNA was diluted to ensure similar amount across treatments, and used to
586 synthesize cDNA with random hexamer primers (Thermo Scientific) and RevertAid reverse
587 transcriptase (Thermo Scientific). The cDNA was then diluted and used as template for
588 qPCR, which was performed with a StepOnePlus™ instrument (Applied Biosystem, USA)
589 and SensiFAST SYBR Hi-ROX Kit (Bioline) according to the manufacturer's instructions.
590 The mRNA levels were normalized to rp49 levels in the same samples. Relative expression
591 values were determined by the $2^{-\Delta\Delta CT}$ method (86). See **Table S1** for the primers used for
592 qPCR.
593
594 ***Crz and Capa Transcript Levels Following Stress***
595 To examine if stress exposure, including desiccation, starvation and chill coma, modified
596 levels of *Crz* and *Capa* transcripts, w^{1118} male flies 6-7 days old were isolated into fresh
597 vials containing enriched medium (with 20-25 flies/vial).
598
599 For desiccation experiments, two out of three vials of flies were transferred to empty vials
600 for 18 hours. After 18 hours of desiccation, flies from one of the empty vials was then
601 transferred into a fresh vial containing moistened compacted Kimwipes (4 wipes with 4mL
602 H_2O) for 4 hours. The remaining two vials, including control flies left in enriched medium for

603 the duration of the experiment and flies desiccated for 18 hours, were sacrificed by plunging
604 in liquid nitrogen and then frozen whole flies were stored at -80°C. Following the 4-hour
605 recovery on moistened Kimwipes of the last vial of flies, the same procedure was done and
606 these flies were sacrificed and stored in -80°C freezer.
607
608 For starvation experiments, two out of three vials of flies were transferred to vials containing
609 moistened and compacted Kimwipes for 18 hours. After 18 hours of starvation, one of the
610 two vials of flies with moistened Kimwipes was then transferred into a fresh vial containing
611 enriched medium for 4 hours. The remaining two vials, including control flies left in enriched
612 medium for the duration of the experiment and flies that had been starved for 18 hours,
613 were immediately sacrificed as described above and stored in -80°C freezer. Following the
614 4-hour feeding recovery on enriched medium of the last vial of flies, they were sacrificed
615 and stored in -80°C freezer.
616
617 For chill coma experiments, two out of three vials of flies were transferred to an ice water
618 slurry and maintained at 0°C for 18 hours. After 18 hours of chill-coma, flies from one of the
619 two vials chilled for 18 hours were transferred into a fresh vial containing enriched medium
620 for 4 hours at room temperature. The remaining two vials, including control flies left in
621 enriched medium for the duration of the experiment and flies that had been subjected to
622 chill-coma for 18 hours, were immediately sacrificed as described above and stored in -
623 80°C freezer. Following the 4-hour room temperature recovery of the last vial of flies, they
624 were sacrificed and stored at -80°C. All the above experiments were repeated in three to
625 four biological replicates.
626
627 Total RNA was isolated using the Monarch Total RNA Miniprep Kit (New England Biolabs,
628 Whitby, ON) following manufacturer guidelines, which included gDNA removal. Purified total
629 RNA was quantified on a Synergy 2 Multimode Microplate Reader using a Take3 micro-
630 volume plate (BioTek, Winooski, VT). For cDNA synthesis, 300ng total RNA was used as
631 template to prepare first-strand cDNA using the iScript Reverse Transcription Supermix for
632 RT-qPCR (Bio-Rad, Mississauga, ON) in a total reaction volume of 10 µL. Following the
633 cDNA synthesis reaction, cDNA was diluted 20-fold by adding nuclease-free H_2O (Wisent,
634 St. Bruno, QC, Canada) and samples were then stored at -20°C until ready for analysis
635 using qPCR.

636

637 Transcript abundance of *Crz* and *Capa* in whole fly cDNA samples was quantified using
638 PowerUp SYBR Green Master Mix (Applied Biosystems, Carlsbad, CA) using fast cycling
639 mode on a StepOnePlus Real-Time PCR System (Applied Biosystems, Carlsbad, CA).
640 Cycling conditions involved initial uracil-DNA glycosylase (UDG) at 50°C for 2 minutes,
641 Dual-Lock DNA polymerase activation at 95°C for 2 minutes, followed by 40 cycles of
642 denaturing at 95°C for 3 seconds and combined annealing extension step at 60°C for 30
643 seconds.

644

645 Following the amplification, reactions were assessed by melt curve analysis and products
646 were also visualized by gel electrophoresis and sequence specificity confirmed by Sanger
647 sequencing. Relative expression levels were determined using the $2^{-\Delta\Delta CT}$ method (86) and
648 normalized to transcript abundance of *rp49* used as a reference gene. Primers were
649 designed over exon-exon boundaries when possible, or at minimum were localized on
650 different exons to exclude possible gDNA amplification. See **Table 3** for the primers used
651 for qPCR.

652

653 **Table 3**: Primers used for qPCR.

Primer name	**Sequence 5' to 3'**
CrzR-RNAi knockdown efficiency	
CrzR F	AATCCGGACAAAAGGCTGGG
CrzR R	AGGTGGAAGGCACCGTAGAT
rp49 F	ATCGGTTACGGATCGAACAA
rp49 R	GACAATCTCCTTGCGCTTCT
Crz and Capa transcript levels following stress	
DmCRZ-274F	GGAGCAGCGATCGTAGGC
DmCRZ-532R	ACATTGGGTTCGGCGGATG
DmCAPA-144F	AGTACAGCTGAGACGGACCAC
DmCAPA-392R	CTTCCTCAGCTCGGCGTC
DmRP49-164F	TCGATATGCTAAGCTGTCGCACA
DmRP49-423R	CGACAATCTCCTTGCGCTTCTTG

654

655 Expression profiles were determined using three technical replicates per target and a
656 minimum of three biological replicates. Finally, no reverse transcriptase control and no
657 template control reactions were also conducted to verify primer fidelity and exclude false
658 positives.

659

660 **Capillary feeding (CAFE) assay**

661 A modified capillary feeding (CAFE) assay was used to monitor food intake of individual flies
662 (10, 87). Capillaries were loaded with food comprised of 5% sucrose, 2% yeast extract and
663 0.1% propionic acid. Food consumption was measured daily and the cumulative food intake
664 over 4 days was calculated. The experiment consisted of at least three biological replicates
665 and 10 flies per replicate for each genotype.

666

667 **Defecation assay**

668 To quantify defecation following TRPA1 based thermogenetic activation of CAPA neurons,
669 flies (mixed sex) were kept on food containing bromophenol blue for 24h at 18°C. One hour
670 before the experiments, flies were transferred to a petri dish lined with wet filter paper.
671 Then, each fly was put in a small glass tube at 29°C and video recorded for 60 min.
672 Afterwards, defecation events and feces drops were counted in 5 min intervals. The total
673 fraction of flies defecating, and the total fraction of defecations (individual flies defecated up
674 to six times during the experiment) were calculated.

675

676 **Mining public datasets for expression of genes**

677 FlyAtlas2 database was mined to determine the distribution of *CrzR* in various tissues (88).
678 The expression of *CAPAR* in the different regions of the gut and its cell types was
679 determined using Flygut-*seq* (89).

680

681 **Statistical analyses**

682 ***Statistical Analyses for Peptide Injection Experiments***

683 The peptide injection experiments (chill-coma recovery and desiccation survival) were each
684 repeated on two-three different occasions (all within one month for each experiment). To
685 account for this, time point was included as a factor in the models and was found to be
686 significant in all cases. This suggests that the overall level of response differed among the

687 different time points. The results as presented, show the treatment effects after controlling
688 for the time effect. These analyses were performed in R (v. 3.4.1) (90) using two-way
689 ANOVA and a Cox proportional hazards model (package survival), respectively.
690
691
692 ***Other Experiments***
693 The experimental data presented in bar graphs represent means ± s.e.m. For the data
694 presented in box-and-whisker plots, each individual value has been plotted and the
695 horizontal line represents the median. Unless stated otherwise, one-way analysis of
696 variance (ANOVA) followed by Tukey's multiple comparisons test was used for comparisons
697 between three genotypes and an unpaired *t*-test was used for comparisons between two
698 genotypes. Stress survival data were compared using log-rank test, Mantel-Cox. All
699 statistical analyses were performed using GraphPad Prism and the confidence intervals are
700 included in the figure captions. The imaging data were analysed by a Shapiro-Wilk normality
701 test followed by a paired Wilcoxon signed rank test in R.
702

Acknowledgements

The authors would like to thank Dr. Olga Kubrak and Dr. Shreyas Jois for initial technical help and advice with experimental design. We are grateful to the Bloomington Drosophila Stock Center (NIH P40OD018537), the Vienna Drosophila Resource Center, and Drs. Ian Orchard, Reinhard Predel, Jan Veenstra, Mark Brown, Heinrich Dircksen, Cornelis Grimmelikhuijzen, Stefan Thor, Jae Park and Shireen Davies for providing flies and reagents. Stina Höglund and the Imaging Facility at Stockholm University (IFSU) are acknowledged for maintenance of the confocal microscopes.

712 ## References

713

714 1. Owusu-Ansah E, Perrimon N. Stress signaling between organs in metazoa. Annu Rev Cell
715 Dev Biol. 2015;31:497-522.

716 2. Droujinine IA, Perrimon N. Defining the interorgan communication network: systemic
717 coordination of organismal cellular processes under homeostasis and localized stress. Front
718 Cell Infect Microbiol. 2013;3:82.

719 3. Robertson GL, Shelton RL, Athar S. The osmoregulation of vasopressin. Kidney Int.
720 1976;10(1):25-37.

721 4. Verney E. TheAntidiuretic Hormone and the Factors Which Determine Its Release. Proc Roy
722 Soc, London, s B. 1948;135:25-106.

723 5. Tatar M, Post S, Yu K. Nutrient control of *Drosophila* longevity. Trends Endocrinol Metab.
724 2014;25(10):509-17.

725 6. Nässel DR, Zandawala M. Recent advances in neuropeptide signaling in *Drosophila*, from
726 genes to physiology and behavior. Prog Neurobiol. 2019;179:101607.

727 7. Rajan A, Perrimon N. *Drosophila* as a model for interorgan communication: lessons from
728 studies on energy homeostasis. Dev Cell. 2011;21(1):29-31.

729 8. Fontana L, Partridge L, Longo VD. Extending healthy life span--from yeast to humans.
730 Science. 2010;328(5976):321-6.

731 9. Kapan N, Lushchak OV, Luo J, Nässel DR. Identified peptidergic neurons in the *Drosophila*
732 brain regulate insulin-producing cells, stress responses and metabolism by coexpressed short
733 neuropeptide F and corazonin. Cell Mol Life Sci. 2012;69:4051-66.

734 10. Liu Y, Luo J, Carlsson MA, Nässel DR. Serotonin and insulin-like peptides modulate
735 leucokinin-producing neurons that affect feeding and water homeostasis in *Drosophila*. J Comp
736 Neurol. 2015;523(12):1840-63.

737 11. Nässel DR, Kubrak OI, Liu Y, Luo J, Lushchak OV. Factors that regulate insulin producing
738 cells and their output in *Drosophila*. Front Physiol. 2013;4:252.

739 12. Nässel DR, Vanden Broeck J. Insulin/IGF signaling in Drosophila and other insects: factors
740 that regulate production, release and post-release action of the insulin-like peptides. Cell Mol
741 Life Sci. 2016;73(2): 271-90

742 13. Isabel G, Martin JR, Chidami S, Veenstra JA, Rosay P. AKH-producing neuroendocrine cell
743 ablation decreases trehalose and induces behavioral changes in *Drosophila*. Am J Physiol
744 Regul Integr Comp Physiol. 2005;288(2):R531-8.

745 14. Kubrak OI, Lushchak OV, Zandawala M, Nässel DR. Systemic corazonin signalling
746 modulates stress responses and metabolism in *Drosophila*. Open Biology. 2016;6(11).

747 15. Lee G, Park JH. Hemolymph sugar homeostasis and starvation-induced hyperactivity
748 affected by genetic manipulations of the adipokinetic hormone-encoding gene in *Drosophila*
749 *melanogaster*. Genetics. 2004;167(1):311-23.

750 16. Zhao Y, Bretz CA, Hawksworth SA, Hirsh J, Johnson EC. Corazonin neurons function in
751 sexually dimorphic circuitry that shape behavioral responses to stress in *Drosophila*. PLoS One.
752 2010;5(2):e9141.

753 17. Oh Y, Lai JS, Mills HJ, Erdjument-Bromage H, Giammarinaro B, Saadipour K, et al. A
754 glucose-sensing neuron pair regulates insulin and glucagon in *Drosophila*. Nature.
755 2019;574(7779):559-64.

756 18. Ahmad M, He L, Perrimon N. Regulation of insulin and adipokinetic hormone/glucagon
757 production in flies. Wiley Interdiscip Rev Dev Biol. 2020;9(2):e360.

758 19. Jourjine N, Mullaney BC, Mann K, Scott K. Coupled Sensing of Hunger and Thirst Signals
759 Balances Sugar and Water Consumption. Cell. 2016;166(4):855-66.

760 20. Galikova M, Dircksen H, Nässel DR. The thirsty fly: Ion transport peptide (ITP) is a novel
761 endocrine regulator of water homeostasis in *Drosophila*. PLoS Genet. 2018;14(8):e1007618.

762 21. Tian S, Zandawala M, Beets I, Baytemur E, Slade SE, Scrivens JH, et al. Urbilaterian origin
763 of paralogous GnRH and corazonin neuropeptide signalling pathways. Sci Rep. 2016;6:28788.

764 22. Zandawala M, Tian S, Elphick MR. The evolution and nomenclature of GnRH-type and
765 corazonin-type neuropeptide signaling systems. Gen Comp Endocrinol. 2018;264:64-77.

766 23. Veenstra JA. Does corazonin signal nutritional stress in insects? Insect Biochem Mol Biol.
767 2009;39(11):755-62.

768 24. Boerjan B, Verleyen P, Huybrechts J, Schoofs L, De Loof A. In search for a common
769 denominator for the diverse functions of arthropod corazonin: a role in the physiology of stress?
770 Gen Comp Endocrinol. 2010;166(2):222-33.

771 25. Miyamoto T, Slone J, Song X, Amrein H. A fructose receptor functions as a nutrient sensor
772 in the *Drosophila* brain. Cell. 2012;151(5):1113-25.

773 26. Terhzaz S, Teets NM, Cabrero P, Henderson L, Ritchie MG, Nachman RJ, et al. Insect
774 capa neuropeptides impact desiccation and cold tolerance. Proc Natl Acad Sci U S A.
775 2015;112(9):2882-7.

776 27. MacMillan HA, Nazal B, Wali S, Yerushalmi GY, Misyura L, Donini A, et al. Anti-diuretic
777 activity of a CAPA neuropeptide can compromise *Drosophila* chill tolerance. J Exp Biol.
778 2018;221(Pt 19).

779 28. Lee G, Kim KM, Kikuno K, Wang Z, Choi YJ, Park JH. Developmental regulation and
780 functions of the expression of the neuropeptide corazonin in *Drosophila melanogaster*. Cell
781 Tissue Res. 2008;331(3):659-73.

782 29. Tayler TD, Pacheco DA, Hergarden AC, Murthy M, Anderson DJ. A neuropeptide circuit
783 that coordinates sperm transfer and copulation duration in *Drosophila*. Proc Natl Acad Sci U S
784 A. 2012;109(50):20697-702.

785 30. Kean L, Cazenave W, Costes L, Broderick KE, Graham S, Pollock VP, et al. Two nitridergic
786 peptides are encoded by the gene capability in *Drosophila melanogaster*. Am J Physiol Regul
787 Integr Comp Physiol. 2002;282(5):R1297-307.

788 31. Santos JG, Pollak E, Rexer KH, Molnar L, Wegener C. Morphology and metamorphosis of
789 the peptidergic Va neurons and the median nerve system of the fruit fly, *Drosophila*
790 *melanogaster*. Cell Tissue Res. 2006;326(1):187-99.

791 32. Wegener C, Reinl T, Jansch L, Predel R. Direct mass spectrometric peptide profiling and
792 fragmentation of larval peptide hormone release sites in *Drosophila melanogaster* reveals
793 tagma-specific peptide expression and differential processing. J Neurochem. 2006;96(5):1362-
794 74.

795 33. Zandawala M, Marley R, Davies SA, Nässel DR. Characterization of a set of abdominal
796 neuroendocrine cells that regulate stress physiology using colocalized diuretic peptides in
797 Drosophila. Cell Mol Life Sci. 2018;75(6):1099-115.

798 34. Imura E, Shimada-Niwa Y, Nishimura T, Huckesfeld S, Schlegel P, Ohhara Y, et al. The
799 Corazonin-PTTH Neuronal Axis Controls Systemic Body Growth by Regulating Basal
800 Ecdysteroid Biosynthesis in *Drosophila melanogaster*. Curr Biol. 2020.

801 35. Bader R, Colomb J, Pankratz B, Schrock A, Stocker RF, Pankratz MJ. Genetic dissection of
802 neural circuit anatomy underlying feeding behavior in *Drosophila*: distinct classes of hugin-
803 expressing neurons. J Comp Neurol. 2007;502(5):848-56.

804 36. Helfrich-Forster C. The period clock gene is expressed in central nervous system neurons
805 which also produce a neuropeptide that reveals the projections of circadian pacemaker cells
806 within the brain of *Drosophila melanogaster*. Proc Natl Acad Sci U S A. 1995;92(2):612-6.

807 37. Schoofs A, Hückesfeld S, Schlegel P, Miroschnikow A, Peters M, Zeymer M, et al.
808 Selection of motor programs for suppressing food intake and inducing locomotion in the
809 *Drosophila* brain. PLoS Biol. 2014;12(6):e1001893.

810 38. Schlegel P, Texada MJ, Miroschnikow A, Schoofs A, Huckesfeld S, Peters M, et al.
811 Synaptic transmission parallels neuromodulation in a central food-intake circuit. Elife. 2016;5.

812 39. Melcher C, Pankratz MJ. Candidate gustatory interneurons modulating feeding behavior in
813 the *Drosophila* brain. PLoS Biol. 2005;3(9):e305.

814 40. Renn SC, Park JH, Rosbash M, Hall JC, Taghert PH. A pdf neuropeptide gene mutation
815 and ablation of PDF neurons each cause severe abnormalities of behavioral circadian rhythms
816 in *Drosophila*. Cell. 1999;99(7):791-802.

817 41. Nitabach MN, Taghert PH. Organization of the *Drosophila* circadian control circuit. Curr
818 Biol. 2008;18(2):R84-93.

819 42. Sgourakis NG, Bagos PG, Papasaikas PK, Hamodrakas SJ. A method for the prediction of
820 GPCRs coupling specificity to G-proteins using refined profile Hidden Markov Models. BMC
821 Bioinformatics. 2005;6:104.

822 43. Choi YJ, Lee G, Hall JC, Park JH. Comparative analysis of Corazonin-encoding genes
823 (Crz's) in *Drosophila* species and functional insights into Crz-expressing neurons. J Comp
824 Neurol. 2005;482(4):372-85.

825 44. Davies SA, Huesmann GR, Maddrell SH, O'Donnell MJ, Skaer NJ, Dow JA, et al. CAP2b, a
826 cardioacceleratory peptide, is present in *Drosophila* and stimulates tubule fluid secretion via
827 cGMP. Am J Physiol. 1995;269(6 Pt 2):R1321-6.

828 45. Paluzzi JP. Anti-diuretic factors in insects: the role of CAPA peptides. Gen Comp
829 Endocrinol. 2012;176(3):300-8.

830 46. Rodan AR, Baum M, Huang CL. The *Drosophila* NKCC Ncc69 is required for normal renal
831 tubule function. Am J Physiol Cell Physiol. 2012;303(8):C883-94.

832 47. Sajadi F, Uyuklu A, Paputsis C, Lajevardi A, Wahedi A, Ber LT, et al. CAPA neuropeptides
833 and their receptor form an anti-diuretic hormone signaling system in the human disease vector,
834 *Aedes aegypti*. Sci Rep. 2020;10(1):1755.

835 48. Davies SA, Cabrero P, Povsic M, Johnston NR, Terhzaz S, Dow JA. Signaling by
836 *Drosophila* capa neuropeptides. Gen Comp Endocrinol. 2013;188:60-6.

837 49. Pollock VP, McGettigan J, Cabrero P, Maudlin IM, Dow JA, Davies SA. Conservation of
838 capa peptide-induced nitric oxide signalling in Diptera. J Exp Biol. 2004;207(Pt 23):4135-45.

839 50. Sajadi F, Curcuruto C, Al Dhaheri A, Paluzzi JV. Anti-diuretic action of a CAPA
840 neuropeptide against a subset of diuretic hormones in the disease vector *Aedes aegypti*. J Exp
841 Biol. 2018;221(Pt 7).

842 51. Coast GM, Orchard I, Phillips JE, Schooley DA. Insect diuretic and antidiuretic hormones.
843 Advances in Insect Physiology. 29: Academic Press; 2002. p. 279-409.

844 52. Marron MT, Markow TA, Kain KJ, Gibbs AG. Effects of starvation and desiccation on
845 energy metabolism in desert and mesic *Drosophila*. J Insect Physiol. 2003;49(3):261-70.

846 53. Gibbs AG, Chippindale AK, Rose MR. Physiological mechanisms of evolved desiccation
847 resistance in *Drosophila melanogaster*. J Exp Biol. 1997;200(Pt 12):1821-32.

848 54. Schooley DA, Horodyski FM, Coast GM. 9 - Hormones Controlling Homeostasis in Insects.
849 In: Gilbert LI, editor. Insect Endocrinology. San Diego: Academic Press; 2012. p. 366-429.

850 55. Bergland AO, Chae HS, Kim YJ, Tatar M. Fine-scale mapping of natural variation in fly
851 fecundity identifies neuronal domain of expression and function of an aquaporin. PLoS Genet.
852 2012;8(4):e1002631.

853 56. Miyamoto T, Amrein H. Diverse roles for the *Drosophila* fructose sensor Gr43a. Fly (Austin).
854 2014;8(1):19-25.

855 57. Fujii S, Yavuz A, Slone J, Jagge C, Song X, Amrein H. Drosophila sugar receptors in sweet
856 taste perception, olfaction, and internal nutrient sensing. Curr Biol. 2015;25(5):621-7.

857 58. Root CM, Ko KI, Jafari A, Wang JW. Presynaptic facilitation by neuropeptide signaling
858 mediates odor-driven food search. Cell. 2011;145(1):133-44.

859 59. Ko KI, Root CM, Lindsay SA, Zaninovich OA, Shepherd AK, Wasserman SA, et al.
860 Starvation promotes concerted modulation of appetitive olfactory behavior via parallel
861 neuromodulatory circuits. Elife. 2015;4.

862 60. Martelli C, Pech U, Kobbenbring S, Pauls D, Bahl B, Sommer MV, et al. SIFamide
863 Translates Hunger Signals into Appetitive and Feeding Behavior in Drosophila. Cell Rep.
864 2017;20(2):464-78.

865 61. Yu Y, Huang R, Ye J, Zhang V, Wu C, Cheng G, et al. Regulation of starvation-induced
866 hyperactivity by insulin and glucagon signaling in adult *Drosophila*. Elife. 2016;5.

867 62. Bharucha KN, Tarr P, Zipursky SL. A glucagon-like endocrine pathway in *Drosophila*
868 modulates both lipid and carbohydrate homeostasis. J Exp Biol. 2008;211(Pt 19):3103-10.

869 63. Inagaki HK, Panse KM, Anderson DJ. Independent, reciprocal neuromodulatory control of
870 sweet and bitter taste sensitivity during starvation in *Drosophila*. Neuron. 2014;84(4):806-20.

871 64. Tian S, Egertova M, Elphick MR. Functional Characterization of Paralogous Gonadotropin-
872 Releasing Hormone-Type and Corazonin-Type Neuropeptides in an Echinoderm. Front
873 Endocrinol (Lausanne). 2017;8:259.

874 65. Sha K, Choi SH, Im J, Lee GG, Loeffler F, Park JH. Regulation of ethanol-related behavior
875 and ethanol metabolism by the Corazonin neurons and Corazonin receptor in *Drosophila*
876 *melanogaster*. PLoS One. 2014;9(1):e87062.

877 66. Allan DW, St Pierre SE, Miguel-Aliaga I, Thor S. Specification of neuropeptide cell identity
878 by the integration of retrograde BMP signaling and a combinatorial transcription factor code.
879 Cell. 2003;113(1):73-86.

880 67. Asahina K, Watanabe K, Duistermars BJ, Hoopfer E, Gonzalez CR, Eyjolfsdottir EA, et al.
881 Tachykinin-expressing neurons control male-specific aggressive arousal in *Drosophila*. Cell.
882 2014;156(1-2):221-35.

883 68. Terhzaz S, Cabrero P, Robben JH, Radford JC, Hudson BD, Milligan G, et al. Mechanism
884 and function of *Drosophila* capa GPCR: a desiccation stress-responsive receptor with functional
885 homology to human neuromedinU receptor. PLoS One. 2012;7(1):e29897.

886 69. Choi YJ, Lee G, Park JH. Programmed cell death mechanisms of identifiable peptidergic
887 neurons in *Drosophila melanogaster*. Development. 2006;133(11):2223-32.

888 70. Pfeiffer BD, Truman JW, Rubin GM. Using translational enhancers to increase transgene
889 expression in *Drosophila*. Proc Natl Acad Sci U S A. 2012;109(17):6626-31.

890 71. Chen TW, Wardill TJ, Sun Y, Pulver SR, Renninger SL, Baohan A, et al. Ultrasensitive
891 fluorescent proteins for imaging neuronal activity. Nature. 2013;499(7458):295-300.

892 72. Shafer OT, Kim DJ, Dunbar-Yaffe R, Nikolaev VO, Lohse MJ, Taghert PH. Widespread
893 receptivity to neuropeptide PDF throughout the neuronal circadian clock network of *Drosophila*
894 revealed by real-time cyclic AMP imaging. Neuron. 2008;58(2):223-37.

895 73. Schindelin J, Arganda-Carreras I, Frise E, Kaynig V, Longair M, Pietzsch T, et al. Fiji: an
896 open-source platform for biological-image analysis. Nat Methods. 2012;9(7):676-82.

897 74. Pollak E, Eckert M, Molnar L, Predel R. Differential sorting and packaging of capa-gene
898 related products in an insect. J Comp Neurol. 2005;481(1):84-95.

899 75. Veenstra JA, Davis NT. Localization of corazonin in the nervous system of the cockroach
900 *Periplaneta americana*. Cell Tissue Res. 1993;274(1):57-64.

901 76. Veenstra JA, Agricola HJ, Sellami A. Regulatory peptides in fruit fly midgut. Cell Tissue
902 Res. 2008;334(3):499-516.

903 77. Kaufmann C, Brown MR. Adipokinetic hormones in the African malaria mosquito,
904 *Anopheles gambiae*: Identification and expression of genes for two peptides and a putative
905 receptor. Insect Biochem Molec. 2006;36(6):466-81.

906 78. Grimmelikhuijzen CJP. FMRFamide is generally occuring in the nervous system of
907 coelenterates. Histochemistry. 1983;78:361-81.

908 79. Dircksen H, Zahnow CA, Gaus G, Keller R, Rao KR, Riehm JP. The ultrastructure of nerve
909 endings containing pigmentdispersing hormone (PDH) in crustacean sinus glands: identification
910 by an antiserum against synthetic PDH. Cell Tissue Res. 1987;250:377–87.

911 80. Nässel DR, Cantera R, Karlsson A. Neurons in the cockroach nervous system reacting with
912 antisera to the neuropeptide leucokinin I. J Comp Neurol. 1992;322(1):45-67.

913 81. Cabrero P, Radford JC, Broderick KE, Costes L, Veenstra JA, Spana EP, et al. The Dh
914 gene of *Drosophila melanogaster* encodes a diuretic peptide that acts through cyclic AMP. J
915 Exp Biol. 2002;205(Pt 24):3799-807.

916 82. Park D, Veenstra JA, Park JH, Taghert PH. Mapping peptidergic cells in *Drosophila*: where
917 DIMM fits in. PLoS One. 2008;3(3):e1896.

918 83. Wahedi A, Gade G, Paluzzi JP. Insight Into Mosquito GnRH-Related Neuropeptide
919 Receptor Specificity Revealed Through Analysis of Naturally Occurring and Synthetic Analogs
920 of This Neuropeptide Family. Front Endocrinol (Lausanne). 2019;10:742.

921 84. Folk DG, Han C, Bradley TJ. Water acquisition and partitioning in Drosophila melanogaster:
922 effects of selection for desiccation-resistance. J Exp Biol. 2001;204(Pt 19):3323-31.

923 85. Feng Y, Ueda A, Wu CF. A modified minimal hemolymph-like solution, HL3.1, for
924 physiological recordings at the neuromuscular junctions of normal and mutant *Drosophila*
925 larvae. J Neurogenet. 2004;18(2):377-402.

926 86. Livak KJ, Schmittgen TD. Analysis of relative gene expression data using real-time
927 quantitative PCR and the 2(-Delta Delta C(T)) Method. Methods. 2001;25(4):402-8.

928 87. Ja WW, Carvalho GB, Mak EM, de la Rosa NN, Fang AY, Liong JC, et al. Prandiology of
929 *Drosophila* and the CAFE assay. Proc Natl Acad Sci U S A. 2007;104(20):8253-6.

930 88. Leader DP, Krause SA, Pandit A, Davies SA, Dow JAT. FlyAtlas 2: a new version of the
931 *Drosophila melanogaster* expression atlas with RNA-Seq, miRNA-Seq and sex-specific data.
932 Nucleic Acids Res. 2018;46(D1):D809-D15.

933 89. Dutta D, Dobson AJ, Houtz PL, Glasser C, Revah J, Korzelius J, et al. Regional Cell-
934 Specific Transcriptome Mapping Reveals Regulatory Complexity in the Adult Drosophila Midgut.
935 Cell Rep. 2015;12(2):346-58.

90. R Core Team. R: A language and environment for statistical computing. . R Foundation for Statistical Computing, Vienna, Austria 2017;URL https://www.R-project.org/.

940 ## Figure captions

941

942 **Figure 1: Crz signaling influences osmotic and ionic stresses. (A)** *Crz^{1}-GAL4* driven
943 *Crz-RNAi (1)* causes a significant decrease in anti-Crz staining (corrected total cell
944 fluorescence, CTCF) in the brains of adult *Drosophila* (**** $p < 0.0001$ as assessed by
945 unpaired *t*-test). **(B)** *Crz* knockdown results in a significant delay in recovery from chill-coma
946 and **(C)** increased survival under ionic stress. For **B** and **C**, data are presented as survival
947 curves (**** $p < 0.0001$, as assessed by Log-rank (Mantel-Cox) test). Crz peptide injections
948 *in vivo* influence **(D, E)** chill-coma recovery and **(F)** desiccation survival. **(D)** Low dose (10^{-}
949 ^{9}M) of injected Crz has no effect whereas a high dose (10^{-6}M) of Crz delays chill-coma
950 recovery (** $p < 0.01$, *** $p < 0.001$ as assessed by two-way ANOVA). **(E)** A non-active
951 exogenous peptide (10^{-6}M), non-amidated *Aedes* adipokinetic hormone/corazonin-related
952 peptide (naACP), has no effect on chill-coma recovery (** $p < 0.01$ as assessed by two-way
953 ANOVA). In **D** and **E**, the y-axes (Time) represents the chill-coma recovery time. **(F)** Crz
954 (10^{-6}M) injected flies (red lines) display reduced survival under desiccation compared to
955 control flies (grey lines) injected with saline. Treatment: $p = 0.0003$ as assessed by Cox
956 proportional hazards model. Two independent trials for **E** and three independent trials for **D**
957 and **F** were performed. These trials are indicated using different symbols (circle, triangle
958 and square).

959

960 **Figure 2: CrzR is expressed in CAPA neurons.** *CrzR-GAL4* drives GFP expression in
961 CAPA/pyrokinin (CAPA/PK) producing neurons (labeled with anti-CAPA antibody) in **(A)** the
962 subesophageal zone (SEZ) and **(B)** ventral nerve cord (VNC) of adult males. The three
963 pairs of neurons in the VNC are referred to as Va neurons.

964

965 **Figure 3: Crz inhibits cAMP levels in Va neurons. (A, B)** Neither the application of 10 µM
966 corazonin nor control saline (HL3.1 containing 0.1% DMSO) significantly altered the signal
967 of the cAMP sensor Epac-camps. Under the experimental conditions, intracellular cAMP
968 levels seemed to be rather low, as indicated by the strong and significant increase in the
969 cAMP sensor signal after application of the membrane-permeable adenylyl cyclase activator
970 NKH477 at the end of the control experiment. NKH477, however, failed to induce a
971 significant rise in the cAMP sensor signal in the corazonin experimental group (n=15 cells,
972 N=5 preparations for both experimental and control group). **(C, D)** Co-application of

973 NKH477 with control saline induced a strong increase in cAMP signal. This NKH477-
974 dependent increase was significantly diminished by co-application of corazonin
975 (experimental group: n=23 cells, N = 5 preparations; control group: n=18 cells, N=5
976 experiments). **(E, F)** Application of 10 μM corazonin or control saline did not significantly
977 affect the signal of the calcium sensor GCaMP6m (experimental group: n=25 cells, N=9
978 preparations; control group: n=17 cells, N=6 preparations. The decline of the signal in (E)
979 represents photobleaching; the raw signal without baseline correction is shown. Grey bars
980 in (A, C, E) represent s.e.m.
981
982 **Figure 4: Crz and CAPA peptide and transcript levels following nutritional and**
983 **osmotic stresses. (A, B)** Crz peptide levels in large neurosecretory cells (indicated by
984 white arrows) are lower in desiccated and rewatered flies compared to flies raised under
985 normal conditions ($p < 0.01$, assessed by One-way ANOVA). **(C, D)** CAPA levels are
986 significantly higher in rewatered flies compared to other conditions ($p < 0.0001$, assessed by
987 One-way ANOVA). **(E)** *Crz* transcript levels are unaltered in desiccated and rewatered flies.
988 **(F)** *CAPA* transcript levels are upregulated following desiccation and return to normal levels
989 after rewatering ($p < 0.05$, assessed by One-way ANOVA). **(G)** *Crz* transcript levels are
990 unaltered following chill-coma. **(H)** *CAPA* transcript levels are downregulated following chill-
991 coma and return to normal levels after recovery at room temperature ($p < 0.05$, assessed by
992 One-way ANOVA).
993
994 **Figure 5: *Va-GAL4* and *CAPA-GAL4* driven *CrzR-RNAi* impacts CAPA signaling and**
995 **stress tolerance. (A)** Knockdown of *CrzR* in Va neurons results in decreased CAPA levels,
996 as measured using immunohistochemistry (** $p < 0.01$ as assessed by Mann-Whitney test).
997 **(B)** Thermogenetic TRPA1-driven activation of CAPA neurons in *CAPA* > *TRPA1* flies
998 (n=24) results in reduced defecation compared to *CAPA* > w^{1118} (n=22) and *TRPA1* > w^{1118}
999 (n=21) controls (* $p < 0.05$ as assessed by Friedman rank sum test). *Va-GAL4* driven *CrzR-*
000 *RNAi(1)* results in **(C)** delayed recovery from chill-coma, and **(D)** increased survival under
001 desiccation, **(E)** ionic and **(F)** starvation stress. *CAPA-GAL4* driven *CrzR-RNAi (1)* increases
002 survival under **(G)** desiccation stress but has no impact on **(H)** chill-coma recovery. For **C-H**,
003 data are presented as survival curves (**** $p < 0.0001$, as assessed by Log-rank (Mantel-
004 Cox) test).
005

006

007 **Figure 6: Crz signaling modulates nutrient and osmotic homeostasis. (A)** A proposed
008 model showing the mode of action of Crz in modulating response to starvation leading to
009 increased food search and food ingestion (black arrows). If the fly is exposed to dry
010 starvation there is an acute response to preserve water and antidiuretic peptides (CAPA1
011 and 2) are released (not shown). When the desiccating fly monitors low nutrient levels (later
012 than the response to osmotic stress) the Crz release ensues and the peptide acts to
013 mobilize energy stores to fuel food search. This results in generation of metabolic water and
014 later accumulation of water from the food. Thus, Crz acts on Va neurons to inhibit CAPA
015 release (red arrow) and allow diuresis to reset water homeostasis. **(B)** A schematic showing
016 the location of Crz (red) and CrzR-expressing neurons/cells (yellow), as well as a model
017 proposing how Crz modulates nutritional and osmotic stresses. Crz is released from dorsal
018 lateral peptidergic neurons (DLPs) into the hemolymph and activates its receptor on the fat
019 body and Va neurons. Crz modulates the release of CAPA from Va neurons, which in turn
020 affects chill-coma recovery and desiccation tolerance via its effect on the renal tubules. Note
021 that *CrzR* is also expressed in the antennal lobes; however, these have been excluded from
022 the figure for purposes of clarity. The scheme is based on findings in this study and that of
023 previous reports (14, 17, 25, 26, 43, 55).

024

025

026 ## Supplementary figures

027

028 **S1 Figure: Crz expression in the CNS of adult *Drosophila.*** *Crz^{2}-GAL4* driven GFP and
029 Crz-immunoreactivity is present in **(A)** dorsal lateral peptidergic neurons (DLPs) in the brain
030 and **(B)** two to **(B^{1})** three pairs of male-specific neurons in the abdominal ganglia. **(C)**
031 *Crz^{1}>20X GFP* expression in the brain. Note that the Crz neuron arborizations can be seen
032 in the antennal lobe (position marked with AL).

033

034 **S2 Figure: *CrzR* is expressed in efferent neurons innervating the rectum. (A)** *CrzR-*
035 *GAL4* driven GFP is not expressed in the midgut, hindgut and Malpighian tubules (MTs). **(B)**
036 *CrzR* is weakly expressed in neurons innervating the rectum. White arrows indicate GFP
037 staining in the region, presumably the water-resorbing rectal pads, which does not stain for
038 phalloidin. **(C)** In adults, *CrzR* is not expressed in tissues (hindgut, MTs and rectal pad)
039 associated with ionic and osmotic homeostasis (Data from FlyAtlas 2 (88))

040

041 **S3 Figure: Crz neuron processes superimpose those of *CrzR* expressing cells in the**
042 **adult *Drosophila* CNS. (A, B)** Crz-producing dorsal lateral peptidergic neurons (DLPs)
043 send projections to the pars intercerebralis near a set of *CrzR>GFP* expressing median
044 neurosecretory cells. **(C)** Crz interneuron projections partly overlap *CrzR>GFP* expressing
045 processes in the lateral horn. In **A-C**, note high *CrzR* expression (based on GFP intensity) in
046 the local interneurons innervating the antennal lobe. **(D)** *CrzR-GAL4* drives strong GFP
047 expression in three pairs of neurons in abdominal ganglion. Weak GFP expression is also
048 observed in two pairs of neurons (indicated by a white arrow).

049

050 **S4 Figure: *CrzR* is expressed in DH44 neurons. (A)** *CrzR-GAL4* drives GFP expression
051 in the median neurosecretory cells (MNCs) expressing diuretic hormone 44 (DH44)
052 neuropeptide. **(B)** Higher magnification image of the DH44 MNCs (white box in **A).** Note that
053 the GFP expression in DH44 neurons is weak and variable.

054

055 **S5 Figure: *CrzR* is not expressed in DH31 and Lk neurons.** *CrzR-GAL4* driven GFP is
056 not expressed in diuretic hormone 31 (DH31) neurons of **(A, B)** the brain and **(C)** the ventral
057 nerve cord. **B** shows a higher magnification image of the DH31 neurons surrounding the
058 antennal lobe MNCs (white box in **A).** *CrzR-GAL4* driven GFP is not expressed in leucokinin

059 (Lk) neurons of **(D)** the lateral horn (LHLKs), **(E)** subesophageal zone (SELKs) and **(F)** the
060 abdominal ganglia (ABLKs).
061
062 **S6 Figure: *CrzR* expression in other peptidergic neurons.** *CrzR* is not expressed in **(A)**
063 brain neurosecretory cells expressing *Drosophila* insulin-like peptide 2 (DILP2) and **(B)**
064 adipokinetic hormone (AKH)-producing cells of the corpora cardiaca (CC). *CrzR-GAL4*
065 drives GFP expression in **(C)** Hugin neurons and **(D)** neurons expressing FMRFamide-
066 related peptide in the SEZ. Note that the exact identity of the neuropeptide present in the
067 neurons labelled with FMRFamide antibody is unknown as it cross-reacts with multiple
068 neuropeptides **(E, F)** *CrzR-GAL4* drives GFP expression in sLNv clock neurons labeled with
069 anti-pigment dispersing factor (PDF) antibody. *CrzR>GFP* expression is present in the
070 characteristic dorsal-projecting (DT) axons of the sLNvs.
071
072 **S7 Figure: Interaction between Crz and CAPA neurons. (A)** Crz interneurons in the
073 abdominal ganglion send axon projections in close proximity to Va neurons. *CrzR-GAL4*
074 drives GFP expression in CAPA/pyrokinin (CAPA/PK) producing neurons (labeled with anti-
075 CAPA antibody) in **(B)** the subesophageal zone (SEZ) and **(C)** ventral nerve cord (VNC) of
076 adult females. The three pairs of neurons in the VNC are referred to as Va neurons.
077
078 **S8 Figure: Peptide and transcript levels following stress and knockdown. (A)** Adult
079 flies were either kept under normal conditions, starved, desiccated or rewatered (desiccated
080 and then incubated on 1% aqueous agar) and Crz peptide levels monitored using
081 immunohistochemistry. Crz peptide levels in all Crz neurons (see Figure 4A for
082 representative images) are lower in starved, desiccated and rewatered flies compared to
083 flies raised under normal conditions (* $p < 0.05$, ** $p < 0.01$ as assessed by One-way
084 ANOVA). Starvation and refeeding do not impact **(B)** *Crz* and **(C)** *CAPA* transcript levels.
085 **(D)** *Actin-GAL4* driven *CrzR-RNAi* (two independent RNAi lines) results in efficient
086 knockdown of *CrzR* transcript in whole adult flies compared to control flies (*Actin>w*^{1118}) as
087 tested by qPCR. (** $p < 0.01$ as assessed by One-way ANOVA).
088
089 **S9 Figure: *Va-GAL4* and *CAPA-GAL4* drive GFP expression in CAPA neurons. (A)** *Va-*
090 *GAL4* drives GFP expression in several neurons in the central nervous system, including a
091 pair of CAPA/pyrokinin producing neurons in the SEZ and **(B)** Va neurons in the VNC

092 (labeled with anti-CAPA antibody). **(C)** *CAPA-GAL4* does not drive GFP expression in the
093 CAPA/pyrokinin neurons in the SEZ but it does so in Va neurons in the VNC **(D)**. Only 5
094 neurons are visible in this preparation; however, there are usually 6 neurons in most
095 preparations **(D[1])**. Note that the posterior-most pair of Va neurons send axonal projections
096 into the abdominal nerve (indicated by the white arrow) where they terminate to form
097 neurohemal release sites. The anterior two pairs send axons to a neurohemal plexus in the
098 dorsal neural sheath.
099
100 **S10 Figure: *Va-GAL4* driven *CrzR-RNAi* impacts food intake.** *CrzR* knockdown in Va
101 neurons results in reduced cumulative food intake measured with CAFE assay over 4 days
102 (*** $p < 0.001$, **** $p < 0.0001$ as assessed by One-way ANOVA).
103
104 **S11 Figure: The *CAPA receptor (CAPAR)* is expressed in the adult gut and Malpighian**
105 **tubules.** *CAPAR-GAL4* drives 20X GFP (*pJFRC81-10xUAS-Syn21-myr::GFP-p10*)
106 expression in the adult **(A)** principal cells of the Malpighian tubules as well as in gut
107 muscles. Note the lack of GFP staining in star-shaped stellate cells. **(B)** A schematic of the
108 adult gut and heat map showing expression of *CAPAR* in different regions of the gut (R1 to
109 R5) and its various cell types (VM, visceral muscle; EEC, enteroendocrine cell; EC,
110 enterocyte; EB, enteroblast; ISC, intestinal stem cell; Ep, epithelium. Data was mined using
111 Flygut-*seq* (89). The *CAPAR-GAL4* expression pattern is in agreement with the
112 transcriptomic data.
113
114

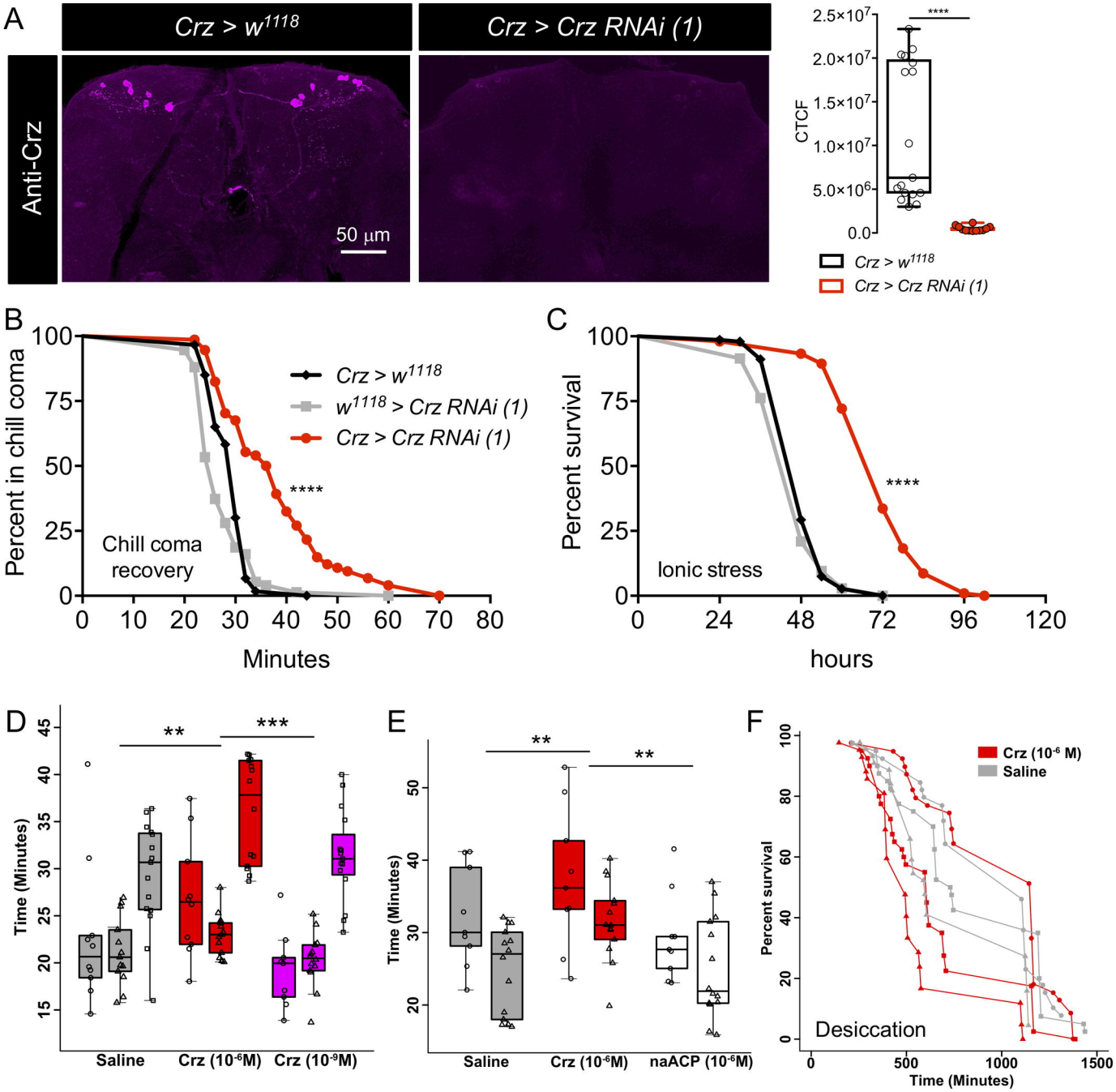
A
Crz > w1118
Crz > Crz RNAi (1)
Anti-Crz
50 µm
CTCF
****
Crz > w1118
Crz > Crz RNAi (1)
B
Percent in chill coma
Chill coma recovery
Crz > w1118
w1118 > Crz RNAi (1)
Crz > Crz RNAi (1)
****
Minutes
C
Percent survival
Ionic stress
****
hours
D
Time (Minutes)
**
***
Saline
Crz (10-6M)
Crz (10-9M)
E
Time (Minutes)
**
**
Saline
Crz (10-6M)
naACP (10-6M)
F
Percent survival
Crz (10-6 M)
Saline
Desiccation
Time (Minutes)

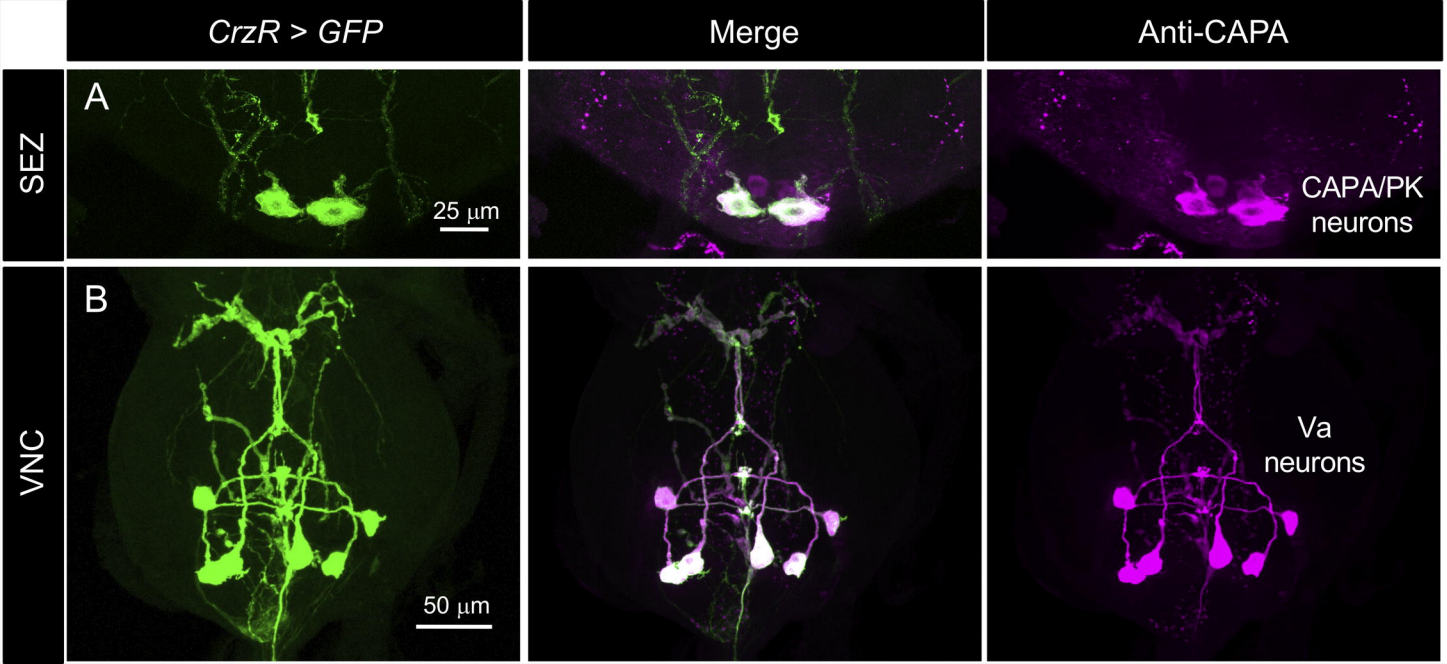
CrzR > GFP
Merge
Anti-CAPA
SEZ
A
25 µm
CAPA/PK
neurons
VNC
B
50 µm
Va
neurons

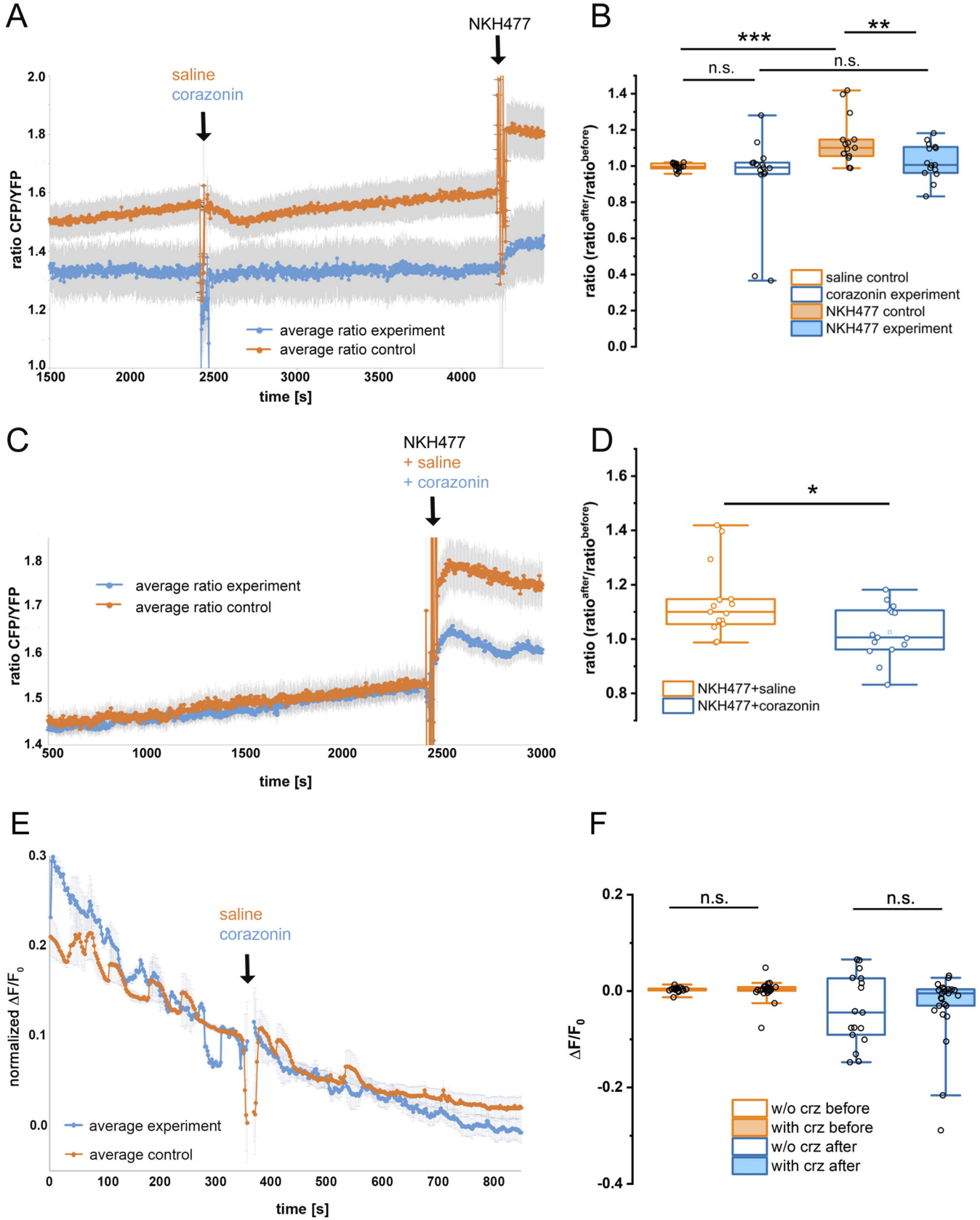
A
NKH477
saline
corazonin
ratio CFP/YFP
average ratio experiment
average ratio control
time [s]
B
***
**
n.s.
n.s.
ratio (ratio^after/ratio^before)
saline control
corazonin experiment
NKH477 control
NKH477 experiment
C
NKH477
+ saline
+ corazonin
ratio CFP/YFP
average ratio experiment
average ratio control
time [s]
D
*
ratio (ratio^after/ratio^before)
NKH477+saline
NKH477+corazonin
E
saline
corazonin
normalized ΔF/F0
average experiment
average control
time [s]
F
n.s.
n.s.
ΔF/F0
w/o crz before
with crz before
w/o crz after
with crz after

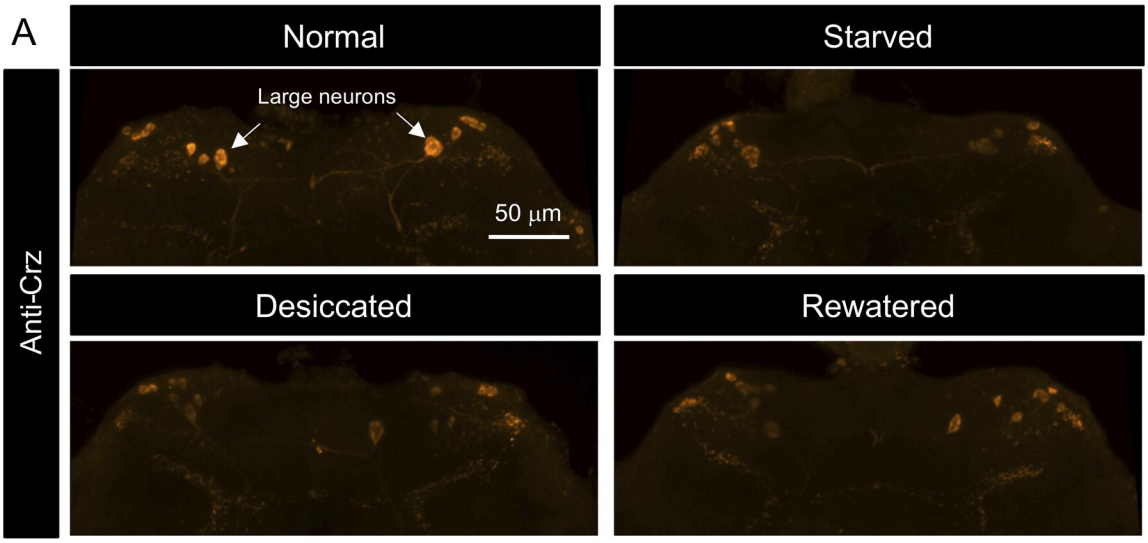
A
Normal
Starved
Desiccated
Rewatered
Anti-Crz
Large neurons
50 µm

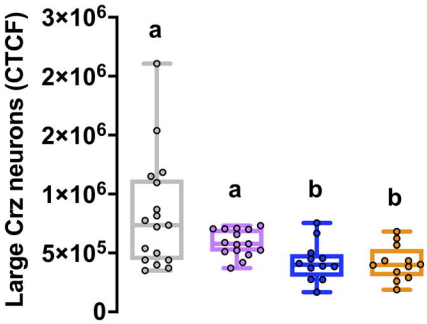
B
Large Crz neurons (CTCF)
3×10^6
2×10^6
2×10^6
1×10^6
5×10^5
0
a
a
b
b

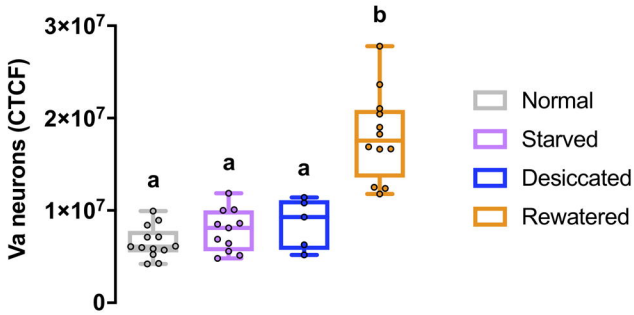
D
Va neurons (CTCF)
3×10^7
2×10^7
1×10^7
0
a
a
a
b
Normal
Starved
Desiccated
Rewatered

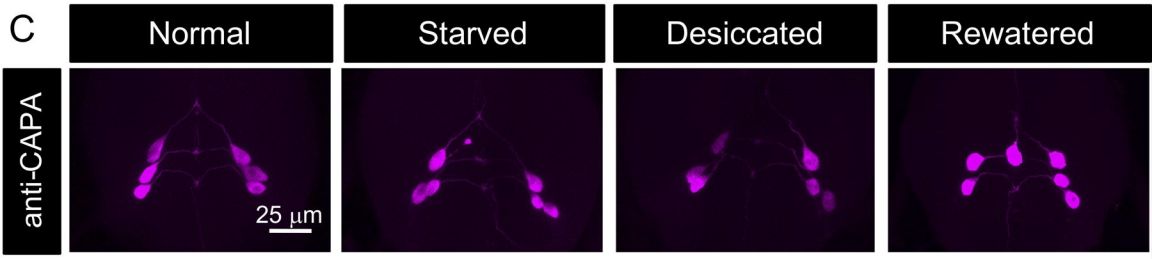
C
Normal
Starved
Desiccated
Rewatered
anti-CAPA
25 µm

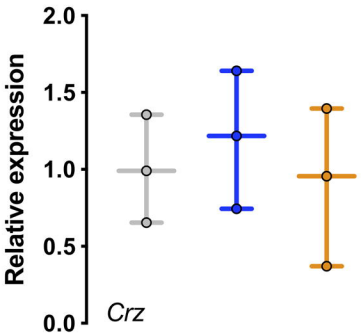
E
Relative expression
2.0
1.5
1.0
0.5
0.0
Crz

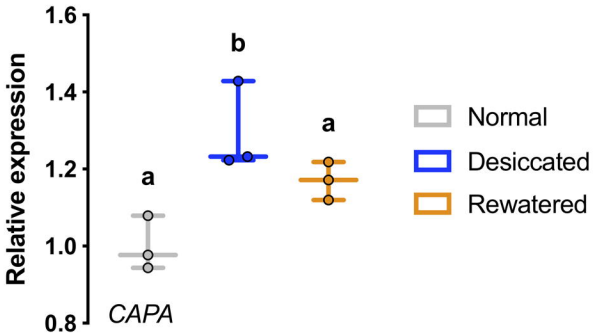
F
Relative expression
1.6
1.4
1.2
1.0
0.8
CAPA
a
b
a
Normal
Desiccated
Rewatered

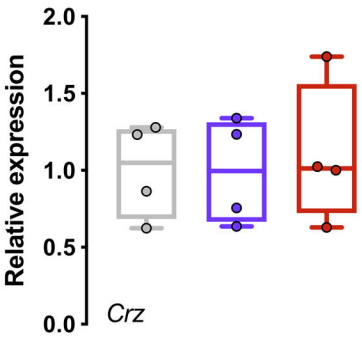
G
Relative expression
2.0
1.5
1.0
0.5
0.0
Crz

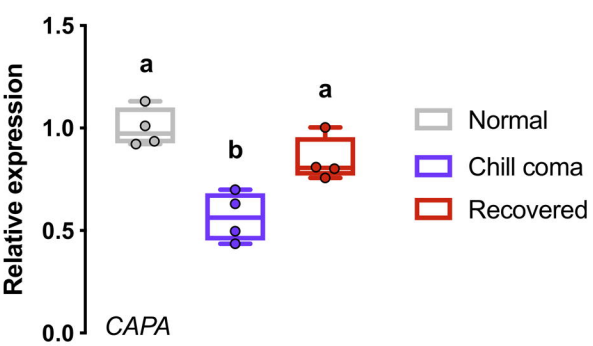
H
Relative expression
1.5
1.0
0.5
0.0
CAPA
a
b
a
Normal
Chill coma
Recovered

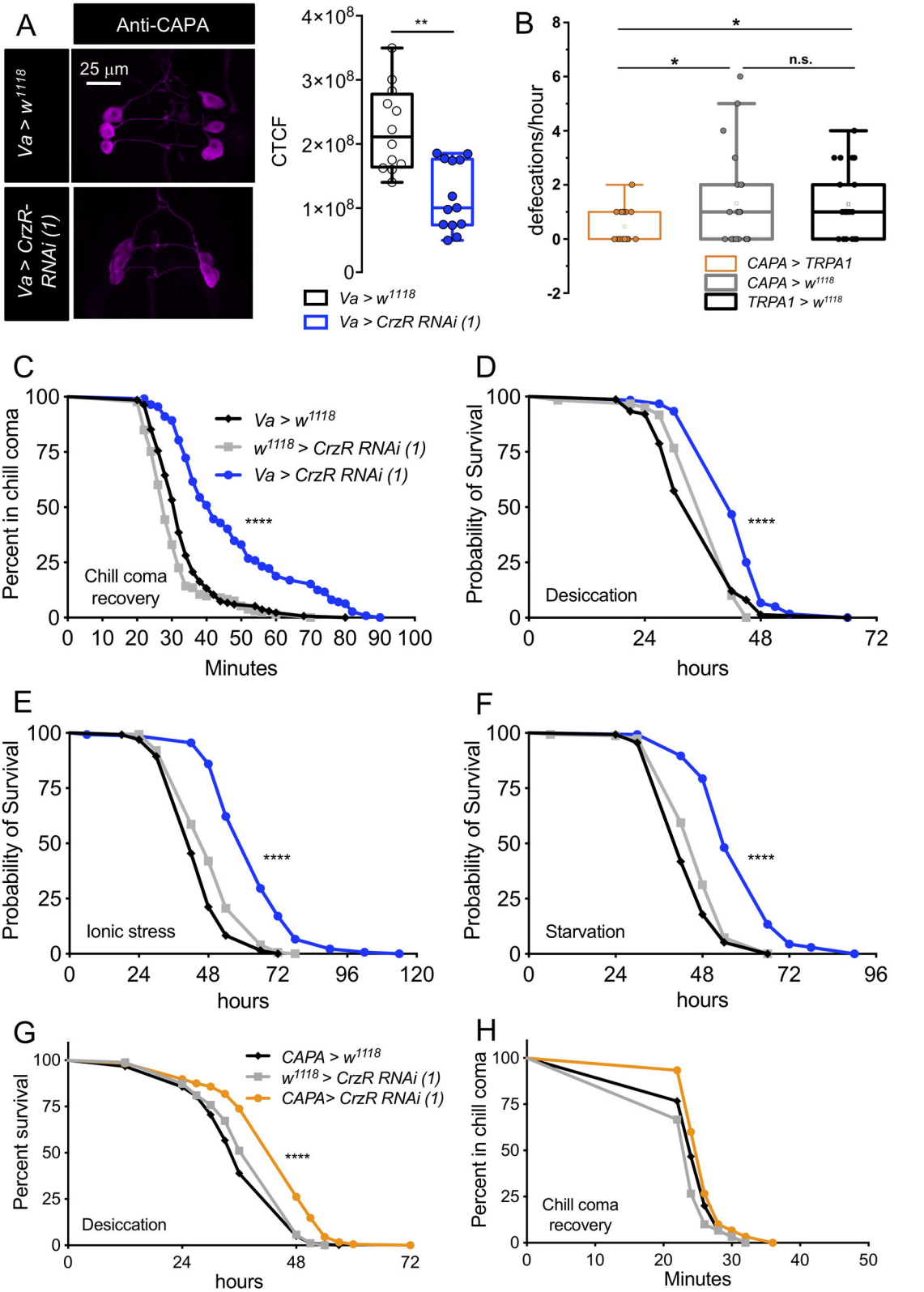
A
Anti-CAPA
25 µm
Va > w1118
Va > CrzR-RNAi (1)
CTCF
4×10^8
3×10^8
2×10^8
1×10^8
0
**
Va > w1118
Va > CrzR RNAi (1)
B
defecations/hour
8
6
4
2
0
-2
*
*
n.s.
CAPA > TRPA1
CAPA > w1118
TRPA1 > w1118
C
Percent in chill coma
Va > w1118
w1118 > CrzR RNAi (1)
Va > CrzR RNAi (1)
****
Chill coma recovery
Minutes
D
Probability of Survival
****
Desiccation
hours
E
Probability of Survival
****
Ionic stress
hours
F
Probability of Survival
****
Starvation
hours
G
Percent survival
CAPA > w1118
w1118 > CrzR RNAi (1)
CAPA> CrzR RNAi (1)
****
Desiccation
hours
H
Percent in chill coma
Chill coma recovery
Minutes

A

Nutrient stress sensed by or relayed to Crz neurons (DLPs)

↓

Crz released from neurosecretory cells (DLPs)

↓

Crz stimulates food search to regain homeostasis, and mobilizes carbohydrate and lipid stores to fuel locomotion

↓

Crz increases feeding to replenish depleted nutrient stores

B

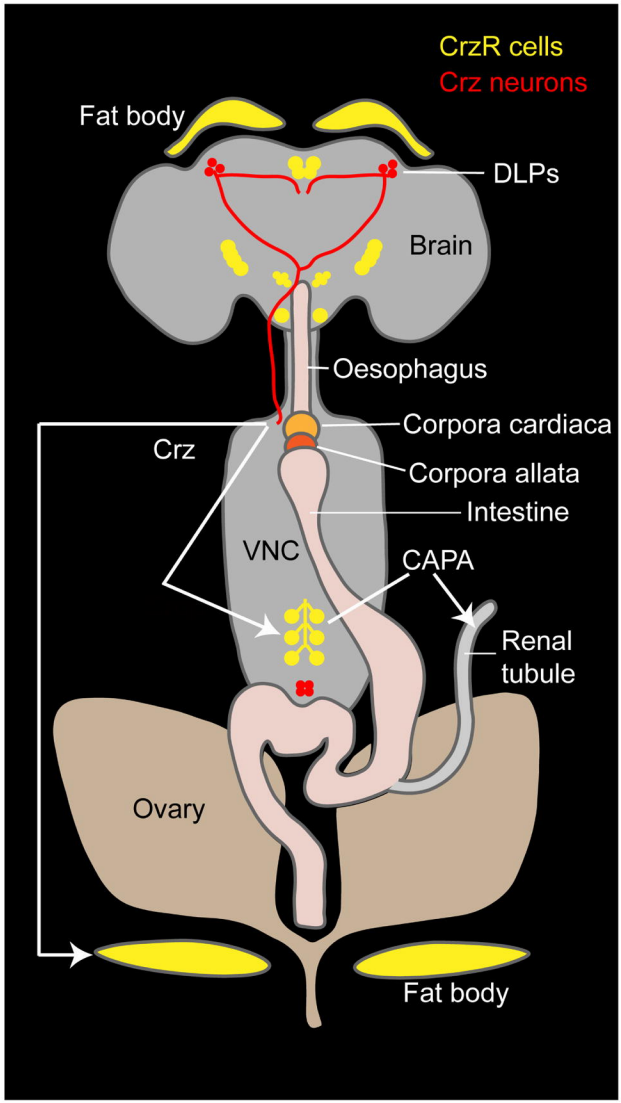

Energy mobilization and food intake:
Crz inhibits CAPA release to reset water homeostasis